STOCHASTIC REDUCTION METHOD FOR BIOLOGICAL CHEMICAL KINETICS USING TIME-SCALE SEPARATION

CHETAN D. PAHLAJANI[1,2], PAUL J. ATZBERGER[2,3], AND MUSTAFA KHAMMASH[3]

Abstract. Many processes in cell biology encode and process information and enact responses by modulating the concentrations of biological molecules. Such modulations serve functions ranging from encoding and transmitting information about external stimuli to regulating internal metabolic states. To understand how such processes operate requires gaining insights into the basic mechanisms by which biochemical species interact and respond to internal and external perturbations. One approach is to model the biochemical species concentrations through the van Kampen Linear Noise Equations, which account for the change in biochemical concentrations from reactions and account for fluctuations in concentrations. For many systems, the Linear Noise Equations exhibit stiffness as a consequence of the chemical reactions occurring at significantly different rates. This presents challenges in the analysis of the kinetics and in performing efficient numerical simulations. To deal with this source of stiffness and to obtain reduced models more amenable to analysis, we present a systematic procedure for obtaining effective stochastic dynamics for the chemical species having relatively slow characteristic time scales while eliminating representations of the chemical species having relatively fast characteristic time scales. To demonstrate the applicability of this multiscale technique in the context of Linear Noise Equations, the reduction is applied to models of gene regulatory networks. Results are presented which compare numerical results for the full system to the reduced descriptions. The presented stochastic reduction procedure provides a potentially versatile tool for systematically obtaining reduced approximations of Linear Noise Equations.

Key words. Stochastic Mode Reduction, Linear Noise Approximation, Gene Regulation, Concentration Fluctuations, Singular Perturbation.

1. Introduction. Many processes in cell biology encode and process information and enact responses by modulating the concentrations of biological molecules. Such modulations serve functions ranging from encoding and transmitting information about external stimuli to regulating internal metabolic states [4, 1]. To understand how such processes operate requires gaining insights into the basic mechanisms by which biochemical species interact and respond to internal and external perturbations. Biological systems pose a number of challenges to modeling since particular species of biological molecules are often present in rather low concentrations, are distributed in space inhomogeneously, and are subject both to passive diffusion and to active transport processes [4, 1, 29, 28, 16].

As an initial approach to understanding how cellular processes modulate biochemical concentrations, many mathematical models have been formulated at a mechanistic level [11, 30, 1, 2]. Models attempt to account phenomenologically for aggregate biochemical kinetics and interrelationships homogenized over the spatial distribution of chemical species and transport processes [4, 1, 16]. The low concentrations of biochemical species also requires accounting for fluctuations, which arise as a consequence of the discrete interactions between biomolecules [1, 2, 10].

To account phenomenologically for these effects, a widely used approach is to draw on models developed for reaction chambers and the chemical kinetics of well-mixed homogeneous systems [11, 30, 1, 12]. A prominent description used for this purpose is the Chemical Master Equation [11, 30]. The Chemical Master Equation keeps track of the number of biomolecules of each chemical species and accounts for the change in number for each individual biochemical reaction which occurs. We discuss this approach in more detail in Section 2. While not always quantitatively accurate for biological systems, such approaches have yielded useful qualitative insights into potential mechanisms underlying biochemical modulation in cellular processes [1, 2, 22].

In practice, the Chemical Master Equation presents for many systems a rather complicated description for analysis and a computationally expensive approach for simulation. In part, this arises since the states of the model depend on the exact number of biochemical molecules of each chemical species and requires updating the state for each chemical reaction event occurring between species. To obtain a more tractable

[1] *Corresponding Author*: University of California at Santa Barbara, 6701 South Hall, Santa Barbara, CA 93106; *E-mail:* chetan@math.ucsb.edu. Last update to manuscript was on June 15, 2010; 5:00pm.

[2] Department of Mathematics, University of California Santa Barbara.

[3] Department of Mechanical Engineering, University of California Santa Barbara.

description, the Linear Noise Approximation (van Kampen Approximation) is often invoked to yield a set of approximating stochastic differential equations which account for the evolution of the biochemical concentrations [30, 8].

For many systems, the chemical reactions occur at significantly different rates. This results in Linear Noise Equations exhibiting stiffness, which presents a challenge for efficient simulation. As a motivating example, consider gene regulation in *Escherichia coli* where the time scale for mRNA transcription is on the order of minutes while the time scale for protein degradation/dilution is on the order of an hour [1]. This suggests that the protein concentrations do not depend strongly on the instantaneous number of mRNAs but rather on an average over time of the number of mRNA molecules. This further suggests that studies of protein concentrations may be possible through a reduced description of the model which eliminates explicit representation of the mRNA concentration from the model, while accounting for such changes in mRNA concentrations through effective terms in the kinetics of the protein species.

We present a systematic approach to obtain such reduced models. The reduced model is obtained by explicitly representing the chemical species having dynamics with relatively slow characteristic time scales while eliminating representations of the chemical species having dynamics with relatively fast characteristic time scales. This has been explored for Kinetic Monte Carlo simulations [13, 25, 6] and for Chemical Master Equation finite state approximations [23, 7]. Here we present a systematic approach to obtaining reduced models of stochastic differential equation descriptions of chemical reactions. Effective stochastic dynamics for the slow chemical species is obtained through a singular perturbation analysis of the Backward Kolomogorov PDEs for the Linear Noise Equations [21, 15, 14, 18]. We discuss this approach in detail in Section 4.

To demonstrate the applicability of this multiscale technique in the context of Linear Noise Equations, the reduction is applied to models of gene regulatory networks. Results are presented which compare numerical results for the full system to the reduced descriptions. These results are presented in Section 7.1. The stochastic reduction procedure presented here provides a potentially versatile tool for systematically obtaining reduced approximations of Linear Noise Equations.

2. Modeling of the Chemical Kinetics. To account phenomenologically for the interactions between biological molecules, a widely used approach is to draw on models developed for reaction chambers and the chemical kinetics of well-mixed homogeneous systems [1, 12]. In this approach the chemical interactions should be thought of as homogenized over the spatial distribution and transport processes within the cell. A prominent description used for this purpose is the Chemical Master Equation [11, 30].

In this approach the biological system is treated as a Markov Chain [27] with states defined by the numbers of biological molecules of each chemical species. The chemical reactions which occur between these chemical species are modeled by state transitions in the Markov Chain. The transitions model the change in the number of each type of biological molecule in accordance to the stoichiometry of the chemical reaction, see Figure 2.1. The Chemical Master Equation governs the time evolution of the probability for observing the Markov Chain in a given state at a given time.

The state of the Markov Chain at time t can be expressed as

$$\mathbf{X}(t) = (X_1(t), X_2(t), X_3(t), \ldots, X_M(t)) \tag{2.1}$$

where X_i is a non-negative integer value. The transition rates between state $\mathbf{X}$ and $\mathbf{Y}$ can be expressed as

$$\mathbf{X} \rightarrow_{\mathbf{a}} \mathbf{Y}, \tag{2.2}$$

where $\mathbf{a} = \mathbf{a}_{\mathbf{X},\mathbf{Y}}$ is the transition rate from state $\mathbf{X}$ to state $\mathbf{Y}$.

The chemical reactions are denoted by R_k for the k^{th} type. The stoichiometry of the reaction is denoted by $\boldsymbol{\nu}^k = (\nu_1^k, \nu_2^k, \nu_3^k, \ldots, \nu_M^k)$. The transitions for this reaction are then from the state $\mathbf{X}$ to the state $\mathbf{Y} = \mathbf{X} + \boldsymbol{\nu}^{(k)}$.

The Chemical Master Equation is

$$\frac{d\mathbf{p}}{dt} = A\mathbf{p}. \tag{2.3}$$

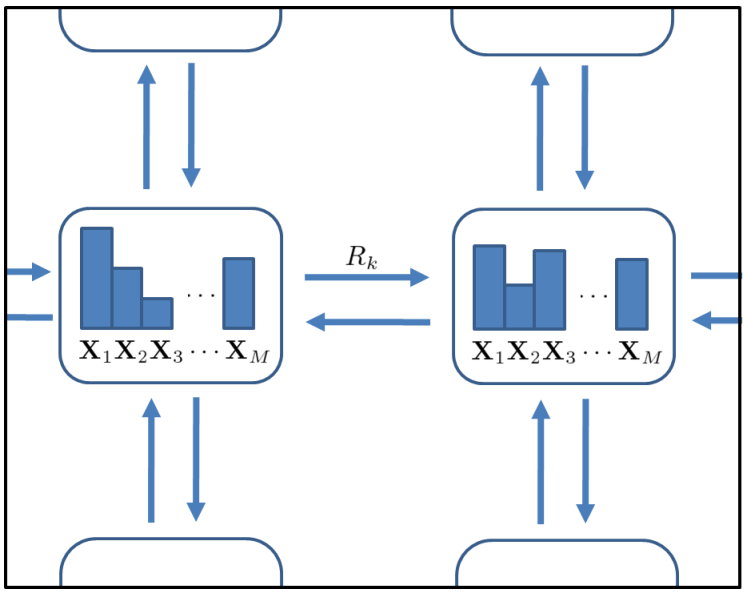

FIG. 2.1. *Markov Chain Model for Chemical Kinetics. The states of the Markov Chain are defined by the numbers of biological molecules of each chemical species, labeled* $X_1, X_2, \cdots, X_M$. *Transitions between these states model the individual chemical reactions which may occur. The transition corresponding to the chemical reaction of type* k *is labeled by* R_k.

The $\mathbf{p}$ denotes the composite vector of probabilities for each possible state of the system. The component corresponding to the state $\mathbf{X}$ is given by $\mathbf{p}_{\mathbf{X}}(t) = \Pr\{\mathbf{X}(t) = \mathbf{X}\}$. The A is the matrix of transition intensities with entries $\mathbf{A}_{\mathbf{X},\mathbf{Y}} = \mathbf{a}_{\mathbf{X},\mathbf{Y}}$.

In general, solving the Chemical Master Equation directly involves computing non-negligible probabilities distributed over a very large number of states. This presents a very high dimensional problem. In practice, an ensemble of stochastic trajectories is often generated to estimate statistical quantities using the Monte-Carlo approach [20]. This requires obtaining realizations of an inhomogeneous Poisson process [27]. This is potentially computationally expensive since each chemical reaction event must be resolved explicitly in the stochastic trajectory.

To circumvent this issue, approximations to the Poisson process using Gaussian processes are utilized. The Linear Noise Approximation provides one such approximation for the concentrations of the chemical species

$$\mathbf{C}(t) = \frac{\mathbf{X}(t)}{n} \approx \mathbf{x}(t) + \frac{1}{\sqrt{n}}\mathbf{V}(t). \tag{2.4}$$

The $\mathbf{C}$ denotes the composite vector of concentrations with the i^{th} component the concentration of the i^{th} chemical species. The n denotes the volume over which the chemical system is homogenized, $\mathbf{x}(t)$ denotes a deterministic function accounting for the mean concentration at time t, and $\mathbf{V}(t)$ denotes a Gaussian stochastic process accounting for concentration fluctuations at time t. This approximation holds in the limit as n is made large while the concentrations are held fixed [11, 30].

Formally, expressions for $\mathbf{x}(t)$ and $\mathbf{V}(t)$ can be obtained by expressing $\mathbf{X}$ in terms of the random time change equation

$$\mathbf{X}(t) = \mathbf{X}(0) + \sum_{k=1}^{N} \boldsymbol{\nu}^k Y_k \left(n \int_0^t \beta_k \left(\frac{\mathbf{X}(s)}{n} \right) ds \right) \tag{2.5}$$

where the Y_k's are independent unit rate Poisson processes [9, 27]. The intensities for the transitions in

terms of species concentration for the k^{th} reaction is given by

$$\beta_k(\mathbf{x}) = \frac{\mathbf{a}_k(n\mathbf{x})}{n}. \tag{2.6}$$

By dividing both sides by n we obtain

$$\frac{\mathbf{X}(t)}{n} = \frac{\mathbf{X}(0)}{n} + \sum_{k=1}^{N} \boldsymbol{\nu}^k \frac{1}{n} Y_k \left(n \int_0^t \beta_k \left(\frac{\mathbf{X}(s)}{n} \right) ds \right). \tag{2.7}$$

A form of the Law of Large Numbers (Theorem 11.2.1 in [9]) states that if

$$\mathbf{x}^{\mathsf{init}} = \lim_{n\to\infty} \frac{\mathbf{X}(0)}{n} \text{ exists and is finite} \tag{2.8}$$

then

$$\lim_{n\to\infty} \sup_{0\le t\le T} \left| \frac{\mathbf{X}(t)}{n} - \mathbf{x}(t) \right| = 0, \qquad \mathbb{P}\text{-a.s.} \tag{2.9}$$

for $T < \infty$ and $\mathbf{x}(t)$ a deterministic function. This implies that for large n

$$\mathbf{x}(t) \approx E\left[\frac{\mathbf{X}(t)}{n} \right]. \tag{2.10}$$

A further consequence of this approximation is that

$$E\left[Y_k \left(n \int_0^t \beta_k \left(\frac{\mathbf{X}(s)}{n} \right) ds \right) \right] \approx E\left[Y_k \left(n \int_0^t \beta_k \left(\mathbf{x}(s) \right) ds \right) \right] = n \int_0^t \beta_k \left(\mathbf{x}(s) \right) ds. \tag{2.11}$$

By taking the expectation of both sides of equation 2.7 and using equation 2.10 and 2.11 we have

$$\mathbf{x}(t) = \mathbf{x}^{\mathsf{init}} + \int_0^t \sum_{k=1}^{N} \boldsymbol{\nu}^k \beta_k(\mathbf{x}(s)) ds. \tag{2.12}$$

The next order in the approximation can be obtained by using a form of the Central Limit Theorem (Theorem 11.2.3 in [9]). The theorem states that if

$$\lim_{n\to\infty} \sqrt{n}(\mathbf{X}(0)/n - \mathbf{x}(0)) = \mathbf{v}^{\mathsf{init}} \text{ exists and is finite} \tag{2.13}$$

then

$$\sqrt{n}(\mathbf{X}(t)/n - \mathbf{x}(t)) \Rightarrow \mathbf{V}(t). \tag{2.14}$$

The $\mathbf{V}(t)$ is given by a Gaussian process inhomogeneous in time satisfying

$$\mathbf{V}(t) = \mathbf{v}^{\mathsf{init}} + \int_0^t DF(\mathbf{x}(s))\mathbf{V}(s) ds + \sum_{k=1}^{N} \boldsymbol{\nu}^k \int_0^t \sqrt{\beta_k(\mathbf{x}(s))} dW_k(s). \tag{2.15}$$

The F is defined by

$$F(\mathbf{x}) = \sum_{k=1}^{N} \boldsymbol{\nu}^k \beta_k(\mathbf{x}). \tag{2.16}$$

The $\Rightarrow$ denotes convergence of the probability distribution of the process.

In the notation, DF denotes the matrix representing the gradient (derivative) of F and $\mathbf{W} = (W_1, W_2, \ldots, W_N)$ is a vector valued Brownian motion in N-dimensions where each vector component W_k is an independent standard Brownian motion [21, 11]. Formally, the equation 2.15 can be obtained in a manner similar to the case of equation 2.12 by computing the mean and variance of increments $d\mathbf{V}(t)$, see [3, 8].

From equations 2.12 and 2.15, it follows that $\mathbf{x}(t)$ and $\mathbf{V}(t)$ satisfy the differential equations

$$\begin{aligned} \dot{\mathbf{x}}(t) &= F(\mathbf{x}(t)) \\ \mathbf{x}(0) &= \mathbf{x}^{\mathsf{init}} \end{aligned} \tag{2.17}$$

$$\begin{aligned} d\mathbf{V}(t) &= DF(\mathbf{x}(t))\mathbf{V}(t)dt + \sum_{k=1}^{N} \boldsymbol{\nu}^k \sqrt{\beta_k(\mathbf{x}(t))} dW_k(t) \\ \mathbf{V}(0) &= \mathbf{v}^{\mathsf{init}}. \end{aligned} \tag{2.18}$$

The stochastic differential equations are to be interpreted in the sense of Ito Calculus [21, 11]. The deterministic and stochastic differential equations 2.17 and 2.18 are referred to as the Linear Noise Equations. They are also referred to as the van Kampen Equations. They provide an approximation of the chemical kinetics as modeled by the trajectories of the Markov Chain through equation 2.4. The Linear Noise Equations will be the object of our subsequent analysis.

3. Chemical Kinetics with Separated Time-Scales. For many systems, the Linear Noise Equations exhibit stiffness as a consequence of the chemical reactions occurring at significantly different rates. This poses challenges to analysis of the kinetics and to efficient numerical simulation. This arises from having to resolve the stochastic dynamics on the fastest characteristic time scales of the system. To obtain reduced models more amenable to analysis and numerical approximation, we consider the case when a decomposition of the system can be found into a part depending on the chemical species having dynamics with relatively slow characteristic time scales and a part depending on chemical species having dynamics with fast characteristic time scales.

More precisely, in terms of the chemical species, we consider a decomposition of the form

$$\mathbf{X} = (\mathbf{X}_{\mathsf{s}}, \mathbf{X}_{\mathsf{f}}). \tag{3.1}$$

The $\mathbf{X}_{\mathsf{s}} = (X_1, \ldots, X_{M_{\mathsf{s}}})$ denotes the "slow" chemical species and $\mathbf{X}_{\mathsf{f}} = (X_{M_{\mathsf{s}}+1}, \ldots, X_M)$ denotes the "fast" chemical species. To define the slow and fast chemical species, a decomposition is sought which yields chemical reactions of the form

$$\mathbf{X} \to \mathbf{X} + \boldsymbol{\nu}^k \tag{3.2}$$

where the stoichiometry satisfies

$$\boldsymbol{\nu}_k = \begin{cases} (\nu_1^k, \nu_2^k, \ldots, \nu_{M_{\mathsf{s}}}^k, 0, \ldots, 0) & \text{if } k \in \Lambda_{\mathsf{s}} \\ (0, \ldots, 0, \nu_{M_{\mathsf{s}}+1}^k, \nu_{M_{\mathsf{s}}+2}^k, \ldots, \nu_M^k) & \text{if } k \in \Lambda_{\mathsf{f}} \end{cases}. \tag{3.3}$$

We write

$$\boldsymbol{\nu}^k = (\boldsymbol{\nu}_{\mathsf{s}}^k, \boldsymbol{\nu}_{\mathsf{f}}^k). \tag{3.4}$$

The Λ_{s} denotes the set of indices associated with the slow chemical reactions while the Λ_{f} denotes the set of indices associated with the fast chemical reactions.

Throughout, it will be assumed that the time scales associated with the fast chemical reactions are well separated from the time scales of the slow chemical reactions. More precisely, for the decomposition it is assumed that the reaction rates can be expressed as

$$\beta_k^{\varepsilon} = \begin{cases} \lambda_k(\mathbf{x}) & \text{if } k \in \Lambda_{\mathsf{s}} \\ \frac{1}{\varepsilon}\lambda_k(\mathbf{x}) & \text{if } k \in \Lambda_{\mathsf{f}} \end{cases} \tag{3.5}$$

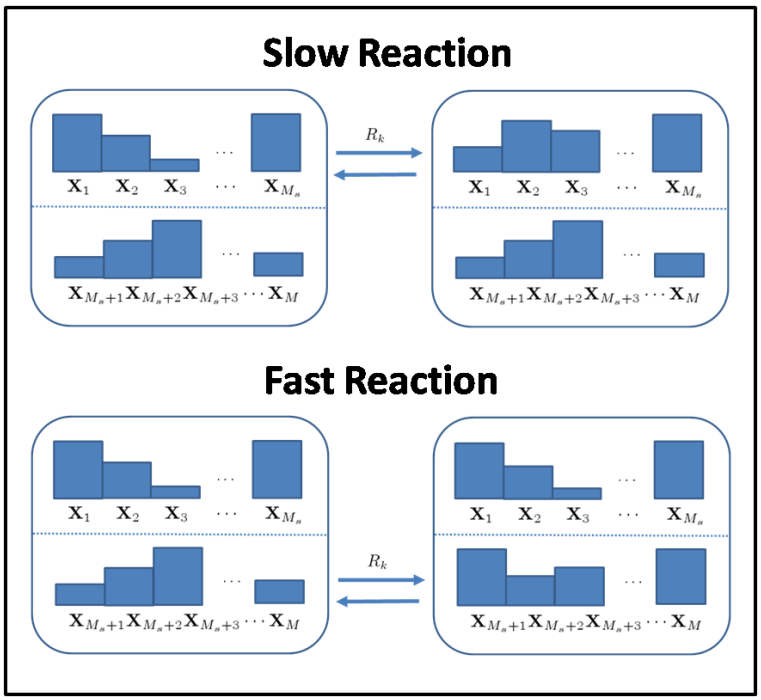

FIG. 3.1. *Slow-Fast Partitioning of the Biochemical Kinetics. A decomposition of the chemical kinetics into fast and slow reactions is sought. The fast reactions correspond to reaction events which are associated with the large transition rates. The slow reactions correspond to reaction events which are associated with the small transition rates. A decomposition is sought which partitions the biochemical species into two disjoint subcollections consistent with the classification of reaction events. While the reaction rates can depend on the number of biological molecules from the full set of biochemical species, the decomposition sought requires the fast reaction events only change the number of biological molecules of one subcollection and the slow reaction events change only the number of biological molecules of the other subcollection.*

where the $\lambda_k(\mathbf{x})$ are order one and ε is small.

This decomposition classifies a chemical species into one of two disjoint subcollections. In the chemical kinetics the decomposition corresponds to the slow reactions involving changes in the number of molecules of chemical species only from the first subcollection while the fast reactions involve changes in the numbers of molecules of chemical species only in the second subcollection. For a schematic of this decomposition, see Figure 3.1. A similar decomposition was used in [7]. In the Linear Noise Approximation, this decomposition corresponds to $\mathbf{x} = (\mathbf{x}_s, \mathbf{x}_f)$ with $\mathbf{x}_s = (x_1, \ldots, x_{M_s})$, $\mathbf{x}_f = (x_{M_s+1}, \ldots, x_M)$, and the stoichiometries $\boldsymbol{\nu}^k$ of equation 3.3.

In practice, such a decomposition may be carried out for generalized chemical species concentrations through use of a change of variable. While this decomposition may seem rather special, we show that such a decomposition arises rather naturally for biological systems in Section 7.1.

4. Stochastic Reduction of the Chemical Kinetics Description : Summary. The Linear Noise Equations can be approximated by a reduced set of equations when the time-scale decomposition holds from Section 3. In this case, the Linear Noise Equations given by equations 2.17 –2.18 can be approximated by the following set of closed Linear Noise Equations expressed solely in terms of the slow degrees of freedom

$$\dot{\mathbf{x}}_s^0(t) = F_s(\mathbf{x}_s^0(t), \mathscr{Z}(\mathbf{x}_s^0(t))) \tag{4.1}$$
$$\mathbf{x}_s^0(0) = \mathbf{x}_s^{\text{init}} \tag{4.2}$$
$$d\mathbf{V}_s^0(t) = B(t)\mathbf{V}_s^0(t)dt + Q(t)d\mathbf{W}(t) \tag{4.3}$$
$$\mathbf{V}_s^0(0) = \mathbf{v}_s^{\text{init}}. \tag{4.4}$$

The operator $\mathscr{Z}$ gives a solution of the implicit equation

$$F_{\mathsf{f}}((\mathbf{x}_{\mathsf{s}}^0(t), \mathscr{Z}(\mathbf{x}_{\mathsf{s}}^0(t))) = 0. \tag{4.5}$$

The drift term in equation 4.3 is given by

$$B(t) = D_{\mathsf{s}}F_{\mathsf{s}} - D_{\mathsf{f}}F_{\mathsf{s}}[D_{\mathsf{f}}F_{\mathsf{f}}]^{-1}D_{\mathsf{s}}F_{\mathsf{f}}. \tag{4.6}$$

Here, F_{s} and F_{f} represent the "slow" and "fast" parts of F:

$$F = \left(F_{\mathsf{s}}, \frac{1}{\varepsilon}F_{\mathsf{f}}\right). \tag{4.7}$$

The D_{s} and D_{f} denote, respectively, the gradients (derivatives) with respect to the variables representing the slow and fast chemical species. The term for the covariance of the stochastic driving process in equation 4.3 is given by

$$[Q(t)]_{i,k} = \nu_i^k \sqrt{\beta_k(\mathbf{x}^0(t))}, \qquad 1 \le i \le M_{\mathsf{s}},\, 1 \le k \le N. \tag{4.8}$$

The notation $[\cdot]_i$ denotes the i^{th} vector component and $[\cdot]_{i,j}$ denotes the i, j matrix entry. In the notation, $B = B(t) = B(\mathbf{x}^0(t))$ and $D_*F_* = D_*F_*(\mathbf{x}^0(t))$ with $\mathbf{x}^0(t) = (\mathbf{x}_{\mathsf{s}}^0(t), \mathscr{Z}(\mathbf{x}_{\mathsf{s}}^0(t)))$.

To motivate how the reduced model given by equations 4.1– 4.4 is obtained, we make a few intuitive remarks. A more rigorous treatment of the derivation is the focus of Section 5. The reduced model is obtained by considering the limit where the fast degrees of freedom relax to statistical steady-state on the characteristic time scales of the slow degrees of freedom. For the deterministic part of the equations, this corresponds to setting

$$\mathbf{x}_{\mathsf{f}}^0(t) = \mathscr{Z}(\mathbf{x}_{\mathsf{s}}^0(t)) = \lim_{r\to\infty} \mathbf{z}(r). \tag{4.9}$$

The $\mathbf{z}(r)$ is the solution of the ODE

$$\dot{\mathbf{z}}(r) = F_{\mathsf{f}}(\mathbf{x}_{\mathsf{s}}(t), \mathbf{z}(r)) \tag{4.10}$$

$$\mathbf{z}(0) = \mathbf{x}_{\mathsf{f}}(t). \tag{4.11}$$

In the case there is an attracting equilibrium solution for the initial condition $\mathbf{z}(0)$, we have $\lim_{r\to\infty} \dot{\mathbf{z}}(r) = 0$. Taking the limit of both sides of equation 4.10 and using continuity of F_{f}, we have that $\mathscr{Z}(\mathbf{x}_{\mathsf{s}}^0(t))$ is a solution of equation 4.5. In the case there is a global attracting equilibrium, the solution of the implicit equation 4.5 is unique.

The motivation for the exact form obtained in equation 4.3 is a little more subtle given the non-differentiability of the stochastic process. Equation 4.3 expresses an averaging of the increments of the full stochastic process consistent with Ito Calculus [21]. The increments are averaged with respect to the invariant probability measure of the fast degrees of freedom. The invariant measure used for this averaging is obtained for each instant in time t by holding fixed the slow degrees of freedom $\mathbf{x}_{\mathsf{s}}$, $\mathbf{V}_{\mathsf{s}}$ and computing the conditional stationary probability measure by allowing $\mathbf{V}_{\mathsf{f}}$ to relax to statistical steady-state. A careful derivation more rigorously establishing this intuition is the focus of Section 5.

5. Derivation of the Stochastic Reduction of the Chemical Kinetics System. A set of reduced Linear Noise Equations of the form given by equations 4.1–4.4 will be derived to approximate the full Linear Noise Equations given by equations 2.17–2.18. The reduced model will be derived using the specific form of the chemical reaction rates given by equation 3.5 and the decomposition discussed in Section 3. This will be used to determine as $\varepsilon \to 0$ the leading order terms approximating the Linear Noise Equations given by equations 2.17–2.18.

5.1. Mean $\mathbf{x}_{\mathsf{s}}^0$. We first compute the leading order terms for the mean behavior of the trajectories to obtain effective equations for $\mathbf{x}_{\mathsf{s}}(t)$. We use the expansion

$$\mathbf{x}^{\varepsilon}(t) = \mathbf{x}^0(t) + \varepsilon \mathbf{x}^1(t) + \varepsilon^2 \mathbf{x}^2(t) + \dots \tag{5.1}$$

which in terms of components is given by

$$x_i^{\varepsilon}(t) = x_i^0(t) + \varepsilon x_i^1(t) + \varepsilon^2 x_i^2(t) + \dots \qquad \text{for } 1 \leq i \leq M. \tag{5.2}$$

Performing a Taylor expansion of the right-hand side of equation 2.17 we have

$$\begin{aligned} F_i(\mathbf{x}^{\varepsilon}(t)) &= F_i(\mathbf{x}^0(t)) + \sum_{k=1}^{M} \frac{\partial F_i}{\partial x_k}(\mathbf{x}^0(t))(x_k^{\varepsilon}(t) - x_k^0(t)) + \mathcal{O}(\varepsilon^2) \\ &= F_i(\mathbf{x}^0(t)) + \varepsilon \sum_{k=1}^{M} \frac{\partial F_i}{\partial x_k}(\mathbf{x}^0(t)) x_k^1(t) + \mathcal{O}(\varepsilon^2). \end{aligned} \tag{5.3}$$

This can be re-expressed in terms of the slow components and fast components using the notation

$$\mathbf{x}_{\mathsf{s}}^{\varepsilon}(t) = \mathbf{x}_{\mathsf{s}}^0(t) + \varepsilon \mathbf{x}_{\mathsf{s}}^1(t) + \dots \tag{5.4}$$

$$\mathbf{x}_{\mathsf{f}}^{\varepsilon}(t) = \mathbf{x}_{\mathsf{f}}^0(t) + \varepsilon \mathbf{x}_{\mathsf{f}}^1(t) + \dots . \tag{5.5}$$

The F can be expressed in the following form using equation 2.16 and the assumptions about the chemical reactions expressed by equations 3.3 and 3.5

$$F = \left(F_s, \frac{1}{\varepsilon} F_f \right) \tag{5.6}$$

$$F_{\mathsf{s}} = \sum_{k \in \Lambda_{\mathsf{s}}} \boldsymbol{\nu}_{\mathsf{s}}^k \beta_k^{\varepsilon}(\mathbf{x}) = \sum_{k \in \Lambda_{\mathsf{s}}} \boldsymbol{\nu}_{\mathsf{s}}^k \lambda_k(\mathbf{x}) \tag{5.7}$$

$$F_{\mathsf{f}} = \varepsilon \sum_{k \in \Lambda_{\mathsf{f}}} \boldsymbol{\nu}_{\mathsf{f}}^k \beta_k^{\varepsilon}(\mathbf{x}) = \sum_{k \in \Lambda_{\mathsf{f}}} \boldsymbol{\nu}_{\mathsf{f}}^k \lambda_k(\mathbf{x}). \tag{5.8}$$

This allows for equation 2.17 to be expanded in terms of slow and fast components as

$$\dot{\mathbf{x}}_{\mathsf{s}}^0(t) + \mathcal{O}(\varepsilon) = F_{\mathsf{s}}(\mathbf{x}_{\mathsf{s}}^0(t), \mathbf{x}_{\mathsf{f}}^0(t)) + \mathcal{O}(\varepsilon) \tag{5.9}$$

$$\dot{\mathbf{x}}_{\mathsf{f}}^0(t) + \mathcal{O}(\varepsilon) = \frac{1}{\varepsilon} F_{\mathsf{f}}(\mathbf{x}_{\mathsf{s}}^0(t), \mathbf{x}_{\mathsf{f}}^0(t)) + \sum_{k=1}^{M} \frac{\partial F_{\mathsf{f}}}{\partial x_k}(\mathbf{x}_{\mathsf{s}}^0(t), \mathbf{x}_{\mathsf{f}}^0(t)) x_k^1(t) + \mathcal{O}(\varepsilon). \tag{5.10}$$

By equating the leading order terms in equation 5.9, which are of order one, we get

$$\dot{\mathbf{x}}_{\mathsf{s}}^0(t) = F_{\mathsf{s}}(\mathbf{x}_{\mathsf{s}}^0(t), \mathbf{x}_{\mathsf{f}}^0(t)). \tag{5.11}$$

By equating the leading order terms in equation 5.10, which are of order $1/\varepsilon$, we obtain

$$F_{\mathsf{f}}(\mathbf{x}_{\mathsf{s}}^0(t), \mathbf{x}_{\mathsf{f}}^0(t)) = 0. \tag{5.12}$$

Solutions of the implicit equation 5.12 can be expressed as

$$\mathbf{x}_{\mathsf{f}}^0(t) = \mathscr{Z}(\mathbf{x}_{\mathsf{s}}^0(t)). \tag{5.13}$$

The equation for the trajectory mean $\mathbf{x}_{\mathsf{s}}^0(t)$ given by equation 4.1 is obtained by substituting equation 5.13 for $\mathbf{x}_{\mathsf{f}}^0(t)$ in equation 5.11. This provides a closed equation for the effective dynamics of the trajectory mean $\mathbf{x}_{\mathsf{s}}^0(t)$.

5.2. Fluctuations $\mathbf{V}_{\mathsf{s}}^0$. We now determine the leading order terms for the fluctuations of the trajectories to obtain effective equations for $\mathbf{V}_{\mathsf{s}}^\varepsilon(t)$. We shall use the Backward Kolomogorov Equation [21, 11]. For the SDEs given by equation 2.18, the Backward Kolomogorov Equation can be expressed as

$$\frac{\partial w^\varepsilon}{\partial t}(t,\mathbf{v}) = (\mathscr{L}^\varepsilon w^\varepsilon)(t,\mathbf{v}) \tag{5.14}$$

$$w^\varepsilon(0,\mathbf{v}) = f(\mathbf{v}) \tag{5.15}$$

with

$$(\mathscr{L}^\varepsilon w)(t,\mathbf{v}) = \sum_{i=1}^{M}[DF(\mathbf{x}^\varepsilon(t))\mathbf{v}]_i \frac{\partial w}{\partial v_i} + \frac{1}{2}\sum_{i,j=1}^{M} a_{ij}^\varepsilon(t)\frac{\partial^2 w}{\partial v_i \partial v_j}. \tag{5.16}$$

For notational convenience we let

$$\sigma_{ik}^\varepsilon = \nu_i^k\sqrt{\beta_k^\varepsilon} \tag{5.17}$$

$$a_{ij}^\varepsilon = \left[\boldsymbol{\sigma}\boldsymbol{\sigma}^T\right]_{ij} = \sum_k \nu_i^k\nu_j^k\beta_k^\varepsilon. \tag{5.18}$$

The Backward Kolomogorov Equation governs statistics of the stochastic process of the form

$$w^\varepsilon(t,\mathbf{v}) = E^{\mathbf{v},0}\left[f(\mathbf{V}^\varepsilon(t))\right]. \tag{5.19}$$

The $E^{\mathbf{v},0}$ denotes expectation over all realizations of the stochastic process with $\mathbf{V}^\varepsilon(0)=\mathbf{v}$. Thus knowledge of the differential operator $\mathscr{L}^\varepsilon$ determines the statistics of the stochastic process. The effective stochastic dynamics for $\mathbf{V}_{\mathsf{s}}^0$ in the limit as $\varepsilon\to 0$ will be obtained by determining the leading order terms in the differential operator $\mathscr{L}^\varepsilon$, which are sufficient to determine the statistics of the stochastic process to leading order.

It is worth remarking that there is a close relationship between the prefactors of the first and second order parts of the differential operator $\mathscr{L}^\varepsilon$ and the stochastic process $\mathbf{V}^\varepsilon(t)$, see [21, 11]. The prefactor of the first order part corresponds to the drift of the stochastic process. The prefactor of the second order part corresponds to the covariance of the stochastic driving field of the process. This relationship can be readily verified for equation 2.18 and 5.16.

The differential operator can be expressed in terms of fast and slow components by defining differential operators $\mathcal{F}^\varepsilon$ and $\mathcal{S}^\varepsilon$ as follows

$$(\mathcal{F}^\varepsilon w)(t,\mathbf{v}) = \sum_{i=M_{\mathsf{s}}+1}^{M}\left[D_{\mathsf{s}}F_{\mathsf{f}}(\mathbf{x}^\varepsilon(t))\mathbf{v}_{\mathsf{s}} + D_{\mathsf{f}}F_{\mathsf{f}}(\mathbf{x}^\varepsilon(t))\mathbf{v}_{\mathsf{f}}\right]_i\frac{\partial w}{\partial v_i} + \frac{1}{2}\sum_{i,j=M_{\mathsf{s}}+1}^{M}\alpha_{ij}^\varepsilon(t)\frac{\partial^2 w}{\partial v_i\partial v_j} \tag{5.20}$$

$$(\mathcal{S}^\varepsilon w)(t,\mathbf{v}) = \sum_{i=1}^{M_{\mathsf{s}}}\left[D_{\mathsf{s}}F_{\mathsf{s}}(\mathbf{x}^\varepsilon(t))\mathbf{v}_{\mathsf{s}} + D_{\mathsf{f}}F_{\mathsf{s}}(\mathbf{x}^\varepsilon(t))\mathbf{v}_{\mathsf{f}}\right]_i\frac{\partial w}{\partial v_i} + \frac{1}{2}\sum_{i,j=1}^{M_{\mathsf{s}}}\alpha_{ij}^\varepsilon(t)\frac{\partial^2 w}{\partial v_i\partial v_j}. \tag{5.21}$$

For convenience, we let

$$\alpha_{ij}^\varepsilon(t) = \sum_k \nu_i^k\nu_j^k\lambda_k(\mathbf{x}^\varepsilon(t)) = \begin{Bmatrix} a_{ij}(\mathbf{x}^\varepsilon(t)) & \text{if } 1\le i,j\le M_{\mathsf{s}} \\ \varepsilon a_{ij}(\mathbf{x}^\varepsilon(t)) & \text{if } M_{\mathsf{s}}+1\le i,j\le M \\ 0 & \text{otherwise.}\end{Bmatrix}. \tag{5.22}$$

The notation $[\cdot]_i$ denotes the i^{th} vector component and $[\cdot]_{i,j}$ denotes the i,j matrix entry.

This allows for the differential operator $\mathscr{L}^\varepsilon$ of the Backward Kolomogorov Equation to be expressed as

$$(\mathscr{L}^\varepsilon w)(t,\mathbf{v}) = \frac{1}{\varepsilon}(\mathcal{F}^\varepsilon w)(t,\mathbf{v}) + (\mathcal{S}^\varepsilon w)(t,\mathbf{v}). \tag{5.23}$$

We now perform a singular perturbation analysis of equation 5.14 using this expression for the differential operator and the expansions

$$w^{\varepsilon}(t,\mathbf{v}) = w_0(t,\mathbf{v}) + \varepsilon w_1(t,\mathbf{v}) + \varepsilon^2 w_2(t,\mathbf{v}) + \dots. \tag{5.24}$$

and

$$\begin{aligned} \mathcal{F}^{\varepsilon} &= \mathcal{F}_0 + \varepsilon\mathcal{F}_1 + \varepsilon^2\mathcal{F}_2 + \dots \\ \mathcal{S}^{\varepsilon} &= \mathcal{S}_0 + \varepsilon\mathcal{S}_1 + \varepsilon^2\mathcal{S}_2 + \dots \end{aligned} \tag{5.25}$$

Our objective is to identify as $\varepsilon \to 0$ an effective operator $\mathscr{L}^0$ for a Backward Kolomogorov Equation satisfied by w_0 depending only on the slow components $\mathbf{v}_{\mathsf{s}}$. This would yield a closed set of stochastic differential equations for the effective stochastic dynamics of the fluctuations $\mathbf{V}_{\mathsf{s}}(t)$.

For the operator $\mathcal{F}^{\varepsilon}$ we shall assume throughout our derivation the following.

Assumption 5.1.

1. *A positive definite matrix is obtained from the entries α_{ij} with indices in the range $M_{\mathsf{s}}+1 \leq i,j \leq M$.*
2. *For $D_{\mathsf{f}}F_{\mathsf{f}}$ considered as a linear operator acting on $\mathbf{v}_{\mathsf{f}} \in \mathbb{R}^{M-M_{\mathsf{s}}}$, each eigenvalue has a real part which is strictly negative.*

These assumptions can be motivated by the requirement of ergodicity of the stochastic process associated with relaxation of the fast components. Further discussion of these conditions will be the focus of Section 6.

By expanding in ε the terms appearing in equations 5.20 and 5.21, we have the leading order terms

$$(\mathcal{F}_0 w)(t,\mathbf{v}) = \sum_{i=M_{\mathsf{s}}+1}^{M} \left[D_{\mathsf{s}}F_{\mathsf{f}}(\mathbf{x}^0(t))\mathbf{v}_{\mathsf{s}} + D_{\mathsf{f}}F_{\mathsf{f}}(\mathbf{x}^0(t))\mathbf{v}_{\mathsf{f}}\right]_i \frac{\partial w}{\partial v_i} + \frac{1}{2}\sum_{i,j=M_{\mathsf{s}}+1}^{M} \alpha_{ij}^0(t)\frac{\partial^2 w}{\partial v_i \partial v_j} \tag{5.26}$$

$$(\mathcal{S}_0 w)(t,\mathbf{v}) = \sum_{i=1}^{M_{\mathsf{s}}} \left[D_{\mathsf{s}}F_{\mathsf{s}}(\mathbf{x}^0(t))\mathbf{v}_{\mathsf{s}} + D_{\mathsf{f}}F_{\mathsf{s}}(\mathbf{x}^0(t))\mathbf{v}_{\mathsf{f}}\right]_i \frac{\partial w}{\partial v_i} + \frac{1}{2}\sum_{i,j=1}^{M_{\mathsf{s}}} \alpha_{ij}^0(t)\frac{\partial^2 w}{\partial v_i \partial v_j}. \tag{5.27}$$

This was obtained by expanding $\mathbf{x}^{\varepsilon}(t)$ using equation 5.1, Taylor expanding F, and by expanding

$$\alpha_{ij}^{\varepsilon} = \alpha_{ij}^0 + \varepsilon\alpha_{ij}^1 + \varepsilon^2\alpha_{ij}^2 + \cdots \tag{5.28}$$

A similar approach can be used for computing the explicit forms of the higher order differential operators, $\mathcal{F}_k$, $\mathcal{S}_k$. However, for our purposes the exact form of the higher order differential operators will not be needed. We shall only use that $\mathcal{F}_1$ is a linear operator that involves first and second partial derivatives only in the components of $\mathbf{v}_{\mathsf{f}}$.

The Backward Kolomogorov Equation given in equation 5.14 can be expressed using the expansions for w^{ε} and $\mathscr{L}^{\varepsilon}$ as

$$\begin{aligned} \frac{\partial w_0}{\partial t} + \varepsilon\frac{\partial w_1}{\partial t} + \dots = &\left(\frac{1}{\varepsilon}\mathcal{F}_0 + \mathcal{F}_1 + \varepsilon\mathcal{F}_2 + \dots\right)(w_0 + \varepsilon w_1 + \dots) \\ &+ \left(\mathcal{S}_0 + \varepsilon\mathcal{S}_1 + \varepsilon^2\mathcal{S}_2 + \dots\right)(w_0 + \varepsilon w_1 + \dots). \end{aligned} \tag{5.29}$$

Equating terms with like powers of ε yields for the first two orders

$$\mathcal{O}(1/\varepsilon) : \mathcal{F}_0 w_0 = 0 \tag{5.30}$$

$$\mathcal{O}(1) : \ \frac{\partial w_0}{\partial t} = \mathcal{F}_0 w_1 + \mathcal{F}_1 w_0 + \mathcal{S}_0 w_0. \tag{5.31}$$

The $\mathcal{O}(1/\varepsilon)$ equation implies that the function w_0 is in the null-space $\mathscr{N}(\mathcal{F}_0)$ of the differential operator $\mathcal{F}_0$,

$$w_0 \in \mathscr{N}(\mathcal{F}_0). \tag{5.32}$$

Under Assumption 5.1, the null-space can be shown to consist only of functions w_0 which are independent of $\mathbf{v_f}$. This means that the functions in the null-space are of the form $w_0 = w_0(t, \mathbf{v_s})$.

Formally, this can be shown from ergodicity of the stochastic processes $\mathbf{Z}_r$ defined by the Backward Kolomogorov Equation with the operator $\mathcal{F}_0$. This gives the stochastic process associated with relaxation of the fast components. For expectations $g(r, \mathbf{v_f}) = E^{\mathbf{v_f},0}[f(\mathbf{Z}_r)]$, the $g_\infty(\mathbf{v_f}) = \lim_{r\to\infty} g(r, \mathbf{v_f})$ satisfies $\mathcal{F}_0 g_\infty = 0$. Any function q in the null-space can be interpreted similarly as a $g_\infty(\mathbf{v_f})$ corresponding to some function f. This follows since f serves as the initial condition of the Kolomogorov Backward Equation and we can set $g(0, \mathbf{v_f}) = f(\mathbf{v_f}) = q(\mathbf{v_f})$ to obtain $g_\infty(\mathbf{v_f}) = \lim_{r\to\infty} e^{r\mathcal{F}_0} q(\mathbf{v_f}) = q(\mathbf{v_f})$. By ergodicity, as $r \to \infty$ the probability distribution of $\mathbf{Z}_r$ relaxes to a stationary distribution independent of the initial condition $\mathbf{Z}_0 = \mathbf{v_f}$. This results in the expectation becoming independent of $\mathbf{v_f}$. As a consequence, $g(r, \mathbf{v_f}) \to g_\infty(\mathbf{v_f}) = g_{\infty,0} = E[f(\mathbf{Z}_\infty)]$, where $g_{\infty,0}$ is a constant independent of $\mathbf{v_f}$. This shows the null-space consists only of functions of the form $w_0 = w_0(t, \mathbf{v_s})$. A more rigorous discussion of the stochastic process $\mathbf{Z}_r$ and its implications for the explicit form taken by the reduced equations is discussed in Section 6.

As a further characterization of how operators act on w_0, we consider $\mathcal{F}_1$, which is an operator that involves partial derivatives with respect to only the components of $\mathbf{v_f}$. This has the consequence that

$$\mathcal{F}_1 w_0 = 0. \tag{5.33}$$

Using this result, the $\mathcal{O}(1)$ condition given by equation 5.31 can be expressed as

$$\mathcal{F}_0 w_1 = \frac{\partial w_0}{\partial t} - (\mathcal{S}_0 w_0). \tag{5.34}$$

For the expansion in w^ε to be valid to order w_1, it is required that the right-hand side be in the range of the differential operator $\mathcal{F}_0$. This gives a solvability condition which must be satisfied by the right-hand side of equation 5.34. This can be expressed as

$$\frac{\partial w_0}{\partial t} - \mathcal{S}_0 w_0 \in \mathscr{R}(\mathcal{F}_0). \tag{5.35}$$

The $\mathscr{R}(\mathcal{F}_0)$ denotes the range of the differential operator $\mathcal{F}_0$. This can also be expressed by requiring

$$\frac{\partial w_0}{\partial t} - \mathcal{S}_0 w_0 \in \mathscr{N}(\mathcal{F}_0^*)^\perp. \tag{5.36}$$

This follows since $\mathscr{R}(\mathcal{F}_0) = \mathscr{N}(\mathcal{F}_0^*)^\perp$, where $\mathcal{F}_0^*$ denotes the adjoint of $\mathcal{F}_0$, see [26].

Under Assumption 5.1, the $\mathscr{N}(\mathcal{F}_0^*)$ is one-dimensional and is spanned by a probability density function of the form $\rho(t, \mathbf{v_s}, \mathbf{v_f})$. The solvability condition given by equation 5.36 can be expressed more explicitly as the orthogonality requirement

$$\int_{\mathbf{v_f}\in\mathbb{R}^{M-M_\mathsf{s}}} \left(\frac{\partial w_0}{\partial t}(t, \mathbf{v_s}) - (\mathcal{S}_0 w_0)(t, \mathbf{v_s}, \mathbf{v_f}) \right) \rho(t, \mathbf{v_s}, \mathbf{v_f}) d\mathbf{v_f} = 0. \tag{5.37}$$

This can be rewritten as

$$\frac{\partial w_0}{\partial t}(t, \mathbf{v_s}) = (\bar{\mathcal{S}}_0 w_0)(t, \mathbf{v_s}) \tag{5.38}$$

$$(\bar{\mathcal{S}}_0 w_0)(t, \mathbf{v_s}) = \int_{\mathbf{v_f}\in\mathbb{R}^{M-M_\mathsf{s}}} (\mathcal{S}_0 w_0)(t, \mathbf{v_s}, \mathbf{v_f}) \rho(\mathbf{v_f}|t, \mathbf{v_s}) d\mathbf{v_f}. \tag{5.39}$$

The conditional probability density is defined by

$$\rho(\mathbf{v_f}|t, \mathbf{v_s}) = \frac{1}{Z} \rho(t, \mathbf{v_s}, \mathbf{v_f}) \tag{5.40}$$

$$Z = \int_{\mathbf{v_f}\in\mathbb{R}^{M-M_\mathsf{s}}} \rho(t, \mathbf{v_s}, \mathbf{v_f}) d\mathbf{v_f}. \tag{5.41}$$

The effective Backward Kolomogorov Equation for $\mathbf{V}_\mathsf{s}$ can then be expressed as

$$\frac{\partial w_0}{\partial t} = \mathscr{L}^0 w_0. \tag{5.42}$$

where $\mathscr{L}^0 = \bar{\mathcal{S}}_0$.

A more explicit form for $\mathscr{L}^0$ can be obtained by performing the averaging of $\mathcal{S}_0$ given in equation 5.39. This yields

$$\mathscr{L}^0 w_0 = \sum_{i=1}^{M_\mathsf{s}} \left[D_\mathsf{s} F_\mathsf{s}(\mathbf{x}^0(t))\mathbf{v}_\mathsf{s} + D_\mathsf{f} F_\mathsf{s}(\mathbf{x}^0(t))\boldsymbol{\mu}(t,\mathbf{v}_\mathsf{s})\right]_i \frac{\partial w_0}{\partial v_i} + \frac{1}{2}\sum_{i,j=1}^{M_\mathsf{s}} \alpha^0_{ij}(t)\frac{\partial^2 w_0}{\partial v_i \partial v_j}(t,\mathbf{v}_\mathsf{s}). \tag{5.43}$$

The $\boldsymbol{\mu}$ denotes the mean value of $\mathbf{V}_\mathsf{f}$ and is defined by

$$\boldsymbol{\mu}(t,\mathbf{v}_\mathsf{s}) = E[\mathbf{V}_\mathsf{f}|\mathbf{v}_\mathsf{s}] = \int_{\mathbf{v}_\mathsf{f}\in\mathbb{R}^{M-M_\mathsf{s}}} \mathbf{v}_\mathsf{f}\rho(\mathbf{v}_\mathsf{f}|t,\mathbf{v}_\mathsf{s})d\mathbf{v}_\mathsf{f}. \tag{5.44}$$

By introducing a little notation, the operator $\mathscr{L}^0$ can be expressed succinctly as

$$\mathscr{L}^0 w_0 = B(t)\mathbf{v}_\mathsf{s}\cdot\nabla_{\mathbf{v}_\mathsf{s}} w_0(t,\mathbf{v}_\mathsf{s}) + \frac{1}{2}\nabla_{\mathbf{v}_\mathsf{s}}\cdot G(t)\nabla_{\mathbf{v}_\mathsf{s}} w_0(t,\mathbf{v}_\mathsf{s}) \tag{5.45}$$

where

$$B(t)\mathbf{v}_\mathsf{s} = D_\mathsf{s} F_\mathsf{s}(\mathbf{x}^0(t))\mathbf{v}_\mathsf{s} + D_\mathsf{f} F_\mathsf{s}(\mathbf{x}^0(t))\boldsymbol{\mu}(t,\mathbf{v}_\mathsf{s}) \tag{5.46}$$

$$[G(t)]_{ij} = \alpha^0_{ij}(t), \qquad 1\le i,j\le M_\mathsf{s} \tag{5.47}$$

$$G = QQ^T. \tag{5.48}$$

In the last equation, Q is used to denote any factor of G. The factor Q can always be defined with real-valued entries as a consequence of Assumption 5.1 condition (1), which ensures that G is positive definite. Any choice of square factors Q_1 and Q_2 are related by a unitary matrix such that $Q_2 = Q_1 U$ for some U with the property $UU^T = I$. As a specific choice for Q, we will use

$$[Q(t)]_{i,k} = \nu_i^k\sqrt{\beta_k(\mathbf{x}^0(t))}, \qquad 1\le i\le M_\mathsf{s},\ 1\le k\le N. \tag{5.49}$$

It can be immediately verified that such a choice yields a Q with the property $G = QQ^T$ by using the definition of G given above and α^0_{ij} given in equations 5.22 and 5.28.

The stochastic process corresponding to the Backward Kolomogorov Equation with operator $\mathscr{L}^0$ gives the effective stochastic dynamics for $\mathbf{V}_\mathsf{s}$ given in equation 4.3. To obtain the specific form for B given in equation 4.3 requires determining the stationary distribution $\rho(\mathbf{v}_\mathsf{f}|t,\mathbf{v}_\mathsf{s})$ and computing explicitly the mean $\boldsymbol{\mu}$. This is the focus of Section 6.

6. Invariant Measure of the Relaxed Stochastic Dynamics of the Fast Components. We now discuss in more detail the specific form taken by the stationary probability density $\rho = \rho(\mathbf{v}_\mathsf{f}|t,\mathbf{v}_\mathsf{s})$ for the invariant measure of the relaxed stochastic dynamics of the fast components. For this purpose, it is useful to consider the stochastic process $\mathbf{Z}_r \in \mathbb{R}^{M-M_\mathsf{s}}$ defined by the Backward Kolomogorov Equation with operator $\mathcal{F}_0$. The probability density of this stochastic process $\rho = \rho(r,\mathbf{v}_\mathsf{f}|t,\mathbf{v}_\mathsf{s})$ is governed by the Forward Kolomogorov Equation

$$\frac{\partial \rho}{\partial r} = \mathcal{F}_0^*\rho. \tag{6.1}$$

The adjoint $\mathcal{F}_0^*$ is given explicitly from equation 5.26 by

$$\begin{aligned}(\mathcal{F}_0^*\rho)(r,\mathbf{v}_\mathsf{f}) = &-\sum_i \frac{\partial}{\partial v_i}\left(\left[D_\mathsf{s} F_\mathsf{f}(\mathbf{x}^0(t))\mathbf{v}_\mathsf{s} + D_\mathsf{f} F_\mathsf{f}(\mathbf{x}^0(t))\mathbf{v}_\mathsf{f}\right]_i \rho(r,\mathbf{v}_\mathsf{f})\right) \\ &+ \frac{1}{2}\sum_{i,j}\alpha^0_{ij}(t)\frac{\partial^2}{\partial v_i\partial v_j}\rho(r,\mathbf{v}_\mathsf{f}).\end{aligned} \tag{6.2}$$

We suppress explicitly notating the conditioning on $t, \mathbf{v}_\mathsf{s}$. For notational convenience we rewrite the adjoint given by equation 6.2 in the form

$$(\mathcal{F}_0^*\rho)(r,\mathbf{v}_\mathsf{f}) = -\nabla_{\mathbf{v}_\mathsf{f}}\cdot(\mathbf{g}\rho(r,\mathbf{v}_\mathsf{f}) + A\mathbf{v}_\mathsf{f}\rho(r,\mathbf{v}_\mathsf{f})) + \frac{1}{2}\nabla_{\mathbf{v}_\mathsf{f}}\cdot\Gamma\nabla_{\mathbf{v}_\mathsf{f}}\rho(r,\mathbf{v}_\mathsf{f}) \tag{6.3}$$

where

$$A = D_\mathsf{f}F_\mathsf{f}(\mathbf{x}^0(t)) \tag{6.4}$$
$$\mathbf{g} = D_\mathsf{s}F_\mathsf{f}(\mathbf{x}^0(t))\mathbf{v}_\mathsf{s} \tag{6.5}$$
$$[\Gamma]_{ij} = \alpha^0_{(M_\mathsf{s}+i)(M_\mathsf{s}+j)}(t), \qquad 1\le i,j\le M-M_\mathsf{s} \tag{6.6}$$
$$\Gamma = RR^T. \tag{6.7}$$

It is important to note that A, $\mathbf{g}$, Γ and R are independent of $\mathbf{v}_\mathsf{f}, r$ and behave with respect to these variables as constants.

In equation 6.7, R is used to denote a factor of Γ which can always be defined with real-valued entries as a consequence of Assumption 5.1 condition (1). The reason for ambiguity in the choice of R is that the Backward Kolomogorov Equation only determines the stochastic process in a weak sense through identifying the probability distribution of the process. In practice, there are many possible stochastic processes having this same probability distribution. Any choice of square factors R_1 and R_2 are related by a unitary matrix so that $R_2 = R_1U$ for some U such that $UU^T = I$. From the invariance of the probability distribution of increments of Brownian motion $d\mathbf{W}(t)$ under unitary transformations U, the stochastic process with driving term $R_1d\mathbf{W}(t)$ has the same probability distribution as the stochastic process with $R_2d\mathbf{W}(t)$.

As a specific choice for R, we shall use

$$[R(t)]_{i,k} = \nu^k_{M_\mathsf{s}+i}\sqrt{\beta_k(\mathbf{x}^0(t))}, \qquad 1\le i\le M-M_\mathsf{s},\ 1\le k\le N. \tag{6.8}$$

It can be immediately verified that such a choice yields R with the property $\Gamma = RR^T$ by using the definition of Γ given in equation 6.6 and α^0_{ij} given in equations 5.22 and 5.28.

We now show formally the ergodicity of the stochastic process corresponding to the Forward Kolomogorov Equation given by equation 6.1. Throughout, we shall use the conditions of Assumption 5.1. This will imply the Forward Kolomogorov Equation given by equation 6.1 has a steady-state solution. The solution is unique when imposing the additional condition that the solution be a probability density.

The Forward Kolomogorov Equation given by equation 6.1 governs the probability distribution $\rho(r,\mathbf{z})$ of the following stochastic process

$$d\mathbf{Z}_r = (\mathbf{g} + A\mathbf{Z}_r)\,dr + Rd\mathbf{W}_r. \tag{6.9}$$

Using the specific form of equation 6.9, the stochastic process can be expressed in terms of Ito Integrals. This is obtained by using the method of integrating factors in Ito Calculus, which yields

$$\mathbf{Z}_r = e^{Ar}\mathbf{Z}_0 + \left[\int_0^r e^{A(r-q)}dq\right]\mathbf{g} + \int_0^r e^{A(r-q)}Rd\mathbf{W}_q \tag{6.10}$$
$$= e^{Ar}\mathbf{Z}_0 - \left[A^{-1}\left(I-e^{Ar}\right)\right]\mathbf{g} - \int_0^r e^{Aq}Rd\mathbf{W}_{r-q}. \tag{6.11}$$

Using properties of the increments of Brownian motion [21, 11], the process $\mathbf{Z}_r$ is equal in probability distribution to the process $\mathbf{Y}_r$ given by

$$\mathbf{Y}_r = e^{Ar}\mathbf{Z}_0 - \left[A^{-1}\left(I-e^{Ar}\right)\right]\mathbf{g} + \int_0^r e^{Aq}Rd\mathbf{W}_q. \tag{6.12}$$

In the limit that $r \to \infty$, we have $e^{Ar} \to 0$ from the properties of A implied by Assumption 5.1. This yields in the limit $r \to \infty$

$$\mathbf{Y}_\infty = -A^{-1}\mathbf{g} + \int_0^\infty e^{Aq} R d\mathbf{W}_q. \tag{6.13}$$

Since $\mathbf{g}$ and A are independent of r, we have from the properties of Ito Integrals [21, 11] that $\mathbf{Y}_\infty$ is a Gaussian random variable.

The conditions appearing in Assumption 5.1 ensure convergence of the Ito Integrals. Independent of the initial condition $\mathbf{Z}_0$, equations 6.10 and 6.12 show as $r \to \infty$ that the distribution of $\mathbf{Z}_r$ approaches a unique stationary probability distribution equal to the distribution of $\mathbf{Y}_\infty$. This demonstrates a form of ergodicity for the stochastic process $\mathbf{Z}_r$.

To use the stationary Gaussian distribution in practice requires determining the mean $\boldsymbol{\mu}$ and covariance C. The mean is obtained by averaging both sides of equation 6.13 to obtain

$$\boldsymbol{\mu} = \langle \mathbf{Y}_\infty \rangle = -A^{-1}\mathbf{g} = -[D_{\mathbf{f}} F_{\mathbf{f}}]^{-1} D_{\mathbf{s}} F_{\mathbf{f}} \mathbf{v}_{\mathbf{s}}. \tag{6.14}$$

This follows since increments of Brownian motion have zero mean $\langle d\mathbf{W}_q \rangle = 0$.

To compute the covariance, we use the Ito Lemma [21, 11] for the process $K_r = \mathbf{Y}_r \mathbf{Y}_r^T$ and equation 6.12 which gives the following stochastic differential equation

$$dK_r = (AK_r + K_r A^T + RR^T)dr + S(r)d\mathbf{W}_r. \tag{6.15}$$

For the covariance term, we have $S(r) = S(r, \mathbf{Y}_r)$, whose precise form we will not need. Averaging both sides of equation 6.15 we obtain

$$dC_r = (AC_r + C_r A^T + RR^T)dr \tag{6.16}$$

where $C_r = \langle K_r \rangle$. This was obtained by using properties of Brownian increments and $\langle d\mathbf{W}_r \rangle = 0$. In the limit $r \to \infty$ we have $dC_r \to 0$ and

$$AC + CA^T = -\Gamma. \tag{6.17}$$

The $C = \lim_{r\to\infty} C_r$ is the equilibrium covariance and $\Gamma = RR^T$ is the covariance of the stochastic driving process. This is often referred to as the fluctuation-dissipation principle, since the expression relates the dissipative operator A to the covariance C of the equilibrium fluctuations and covariance Γ of the stochastic driving process. Under Assumption 5.1, the matrix equation 6.17 can be solved to obtain C.

This yields an approach to obtain explicitly the parameters of the Gaussian equilibrium probability density. This probability density is given by

$$\rho(\mathbf{v}_{\mathbf{f}}|t, \mathbf{v}_{\mathbf{s}}) = \frac{1}{\sqrt{(2\pi)^{(M-M_{\mathbf{s}})} \det(C)}} \exp\left[-\frac{1}{2}(\mathbf{v}_{\mathbf{f}} - \boldsymbol{\mu})^T C^{-1} (\mathbf{v}_{\mathbf{f}} - \boldsymbol{\mu})\right] \tag{6.18}$$

where C is obtained from equation 6.17 and $\boldsymbol{\mu}$ is obtained from equation 6.14.

The effective stochastic equations for the fluctuations $\mathbf{V}_{\mathbf{s}}^0$ given in equation 4.3 are obtained by substituting the mean $\boldsymbol{\mu}$ into equation 5.46 to obtain the specific form of $B(t)$ in equation 4.6. For $R(t)$ appearing in equation 6.7 any factor satisfying $\Gamma = RR^T$ can be used. To represent the stochastic dynamics we used the specific choice given by equation 5.49. This completes the derivation of the effective stochastic equations for the fluctuations $\mathbf{V}_{\mathbf{s}}^0$ given in equation 4.3.

7. Applications.

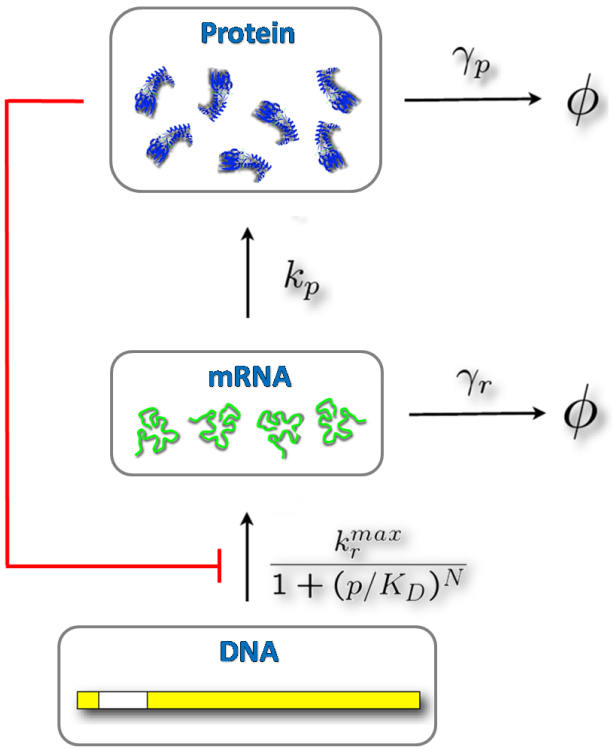

FIG. 7.1. *Autoregulatory Gene Network. A basic autoregulatory gene network is shown which uses negative feedback to maintain the concentration of a protein at a constant level. The basic mechanism consists of the following steps: (i) An RNA-polymerase binds to the DNA promoter site in the cell nucleus and transcribes the genetic code to a messenger RNA molecule (mRNA). (ii) The mRNA molecule is transported out of the nucleus and translated by a ribosome to produce molecules of the encoded protein. (iii) Some of the molecules of the encoded protein are transported back into the nucleus and can act to inhibit the transcription of mRNA by binding to the DNA promoter site. In the autoregulatory mechanism, the strength of the inhibition effect depends on the number of protein molecules able to seek out and successfully bind the promoter site. The mRNA and protein are both subject to degradation or dilution over time. When the number of proteins becomes sufficiently large to achieve significant inhibition of mRNA transcription, the steady-state concentration is achieved.*

7.1. Gene-Protein Regulatory Network. As an application of the stochastic reduction technique we consider the biochemical kinetics of a basic gene regulatory network for the maintenance of a protein at a constant concentration. A rather simple regulatory network having this feature is a single gene which produces through the translation of mRNAs a protein which has an inhibitory feedback on the rate of transcription of the mRNAs for the gene. This is summarized schematically in Figure 7.1.

To model this regulatory network at the level of the Linear Noise Equations the concentration of two biochemical species are tracked $\mathbf{C} = (C_P, C_R)$. The concentration of the protein species is denoted by C_P and the concentration of the mRNA species is denoted by C_R. From the Linear Noise Approximation defined by equation 2.4, the protein and mRNA concentrations are given by

$$C_P(t) \approx p + \frac{1}{\sqrt{n}} U(t) \tag{7.1}$$

$$C_R(t) \approx r + \frac{1}{\sqrt{n}} V(t). \tag{7.2}$$

The p denotes the mean protein concentration and r denotes the mean mRNA concentration. The U denotes fluctuations about the mean protein concentration and V denotes fluctuations about the mean

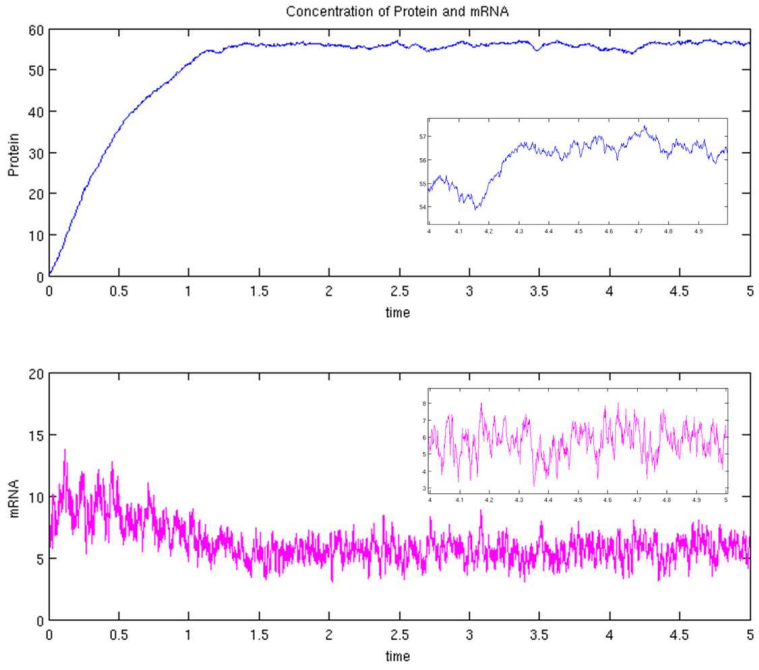

FIG. 7.2. *Protein and mRNA Concentrations. The protein and mRNA concentrations over time are shown for the autoregulatory network modeled by the Linear Noise Equations. The protein and mRNA concentrations exhibit dynamics characterized by distinctly different time-scales. For the protein concentration, the deviations from the mean concentration can be seen to decay over a much longer time scale than for the mRNA concentration. This behavior is further highlighted in the insets.*

mRNA concentration. For more precise definitions see Section 2 and equations 2.10 and 2.15.

As discussed in Section 2, for the Linear Noise Approximation the chemical reaction rates $\mathbf{a}_k$ expressed in terms of the number of molecules of each species must be related to chemical reaction rates expressed in terms of concentrations. Chemical reaction rates β_k for the species concentrations are related to the reaction rates $\mathbf{a}_k$ by

$$\beta_k(\mathbf{x}) = \frac{\mathbf{a}_k(n\mathbf{x})}{n}. \tag{7.3}$$

Here, $\mathbf{x} = (p, r)$ denotes the vector of mean concentrations of the chemical species. It is important that the correspondence given in equation 7.3 be used to relate any parameters in the model obtained from the Linear Noise Approximation to the underlying kinetics given in terms of the numbers of biological molecules.

For the chemical kinetics of the regulatory network, we shall model the rates of the reactions in terms of concentrations by

$$\beta_1 = k_p r, \quad \beta_2 = \gamma_p p, \quad \beta_3 = \tilde{k}_r(p), \quad \beta_4 = \tilde{\gamma}_r r. \tag{7.4}$$

For these reactions, we use the following stoichiometries

$$\boldsymbol{\nu}^1 = (1,0)^T, \quad \boldsymbol{\nu}^2 = (-1,0)^T, \quad \boldsymbol{\nu}^3 = (0,1)^T, \quad \boldsymbol{\nu}^4 = (0,-1)^T. \tag{7.5}$$

Each of the reactions will correspond through equation 7.3 to the production or degradation of a protein molecule or mRNA molecule. From equation 7.3, we see the precise values of the parameters may in fact have dependence on the volume of the domain considered.

The dynamics of the concentrations $C_P(t)$ and $C_R(t)$ are governed by the Linear Noise Equations given by equation 2.18 in Section 2. For the regulatory network, the Linear Noise Equations take the specific form

$$\dot{p} = k_p r - \gamma_p p \tag{7.6}$$

$$\dot{r} = \tilde{k}_r(p) - \tilde{\gamma}_r r \tag{7.7}$$

$$dU(t) = k_p V(t) - \gamma_p U(t)dt + \sqrt{k_p r + \gamma_p p}\; dW_1(t) \tag{7.8}$$

$$dV(t) = \tilde{k}_r'(p)U(t) - \tilde{\gamma}_r V(t)dt + \sqrt{\tilde{k}_r(p) + \tilde{\gamma}_r r}\; dW_2(t) \tag{7.9}$$

$$p(0) = p^{\mathsf{init}}, \quad r(0) = r^{\mathsf{init}}, \quad U(0) = U^{\mathsf{init}}, \quad V(0) = V^{\mathsf{init}}. \tag{7.10}$$

In many bacteria, such as *Escherichia coli*, the time scale for mRNA transcription is on the order of minutes while the time scale for protein degradation/dilution is on the order of an hour. This suggests that the protein concentrations do not depend strongly on the instantaneous number of mRNAs but rather on an average over time of the number of mRNAs. This further suggests that studies of protein concentrations may be possible through a reduced description of the model which eliminates explicit representation of the mRNA concentration from the model, while accounting for such changes in mRNA concentrations through effective terms in the kinetics of the protein species.

For this purpose, we shall use the stochastic reduction techniques introduced in Section 4. To use these formulas in practice, a small parameter ε must be identified for the system. To characterize the disparate time scales of the mRNA and protein response, we use $\varepsilon = \gamma_p/\tilde{\gamma}_r$. Using the small parameter ε, the kinetic terms can be expressed in terms of new terms $k_r(p)$ and γ_r defined by

$$\tilde{k}_r(p) = \frac{1}{\varepsilon} k_r(p) \tag{7.11}$$

$$\tilde{\gamma}_r = \frac{1}{\varepsilon}\gamma_r. \tag{7.12}$$

The ε is used as a prefactor for scaling the parameters of the kinetics of the mRNA to obtain units in which the parameter values k_r, γ_r are comparable in magnitude to k_p, γ_p.

The leading order behavior of the system in ε is captured by the reduced Linear Noise Equations given in Section 4 equation 4.1. To use these results for the regulatory network system requires determining the specific form of the equations for the kinetics given in equation 7.4. From equation 7.4, we have

$$F_{\mathsf{s}}(p, r) = k_p r - \gamma_p p \tag{7.13}$$

$$F_{\mathsf{f}}(p, r) = k_r(p) - \gamma_r r. \tag{7.14}$$

The operator $\mathscr{Z}(p^0)$ is defined by solving $F_{\mathsf{f}}(p^0, \mathscr{Z}(p^0)) = 0$. This gives

$$r^0 = \mathscr{Z}(p^0) = \frac{k_r(p^0)}{\gamma_r}. \tag{7.15}$$

The gradients are given by

$$D_{\mathsf{s}}F_{\mathsf{s}} = -\gamma_p, \quad D_{\mathsf{f}}F_{\mathsf{s}} = k_p \tag{7.16}$$

$$D_{\mathsf{s}}F_{\mathsf{f}} = k_r'(p^0), \quad D_{\mathsf{f}}F_{\mathsf{f}} = -\gamma_r. \tag{7.17}$$

This gives from equations 4.6 and 7.16

$$B = \frac{k_p k_r'(p^0)}{\gamma_r} - \gamma_p. \tag{7.18}$$

From equation 6.6 and 5.22 we have

$$G = \frac{k_p k_r(p^0)}{\gamma_r} + \gamma_p p^0. \tag{7.19}$$

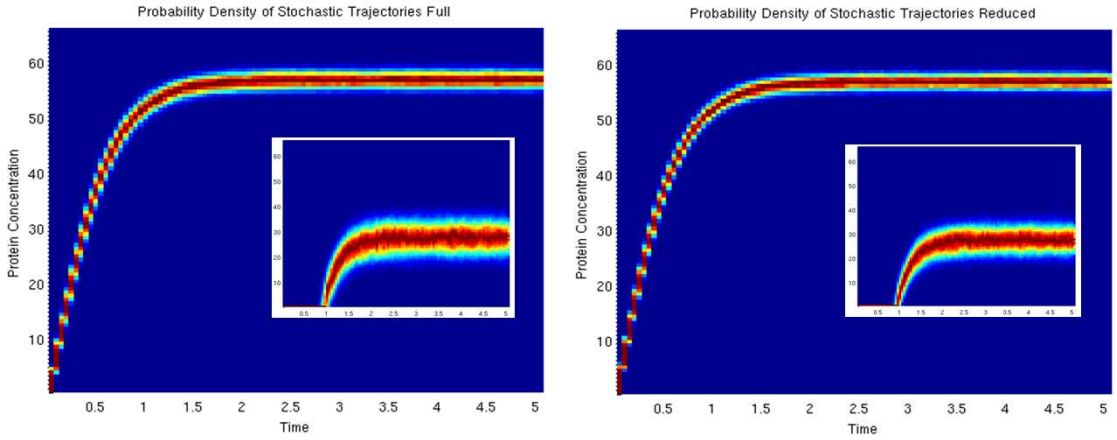

FIG. 7.3. *Comparison of the Full Stochastic Dynamics to Reduced Stochastic Dynamics. The full stochastic dynamics are shown in the case where both the protein and mRNA concentrations are resolved (left panel). The reduced stochastic dynamics are shown in the case where only the protein concentration is resolved explicitly (right panel). The marginal probability density at each time of the protein concentration is shown for an ensemble of trajectories with* $\varepsilon = 10^{-2}$*, all starting with* $p^{\text{init}} = 0, r^{\text{init}} = 0, U^{\text{init}} = 0, V^{\text{init}} = 0$*, and parameter values given in Table 7.2. The protein concentrations are shown in pseudo-color to indicate the probability of being realized by a stochastic trajectory of the system. The marginal probability densities are seen to compare qualitatively well.*

The reduced stochastic dynamics for the protein concentration are obtained by substituting equations 7.13 – 7.19 into equation 4.1.

This gives the reduced Linear Noise Equations for the protein concentration

$$\dot{p^0} = \frac{k_p k_r(p^0)}{\gamma_r} - \gamma_p p^0 \tag{7.20}$$

$$dU^0(t) = \left(\frac{k_p k_r'(p^0)}{\gamma_r} - \gamma_p\right) U^0(t)dt + \sqrt{\frac{k_p k_r(p^0)}{\gamma_r} + \gamma_p p^0}\; dW(t). \tag{7.21}$$

This reduces the four dimensional stochastic dynamical system to only two degrees of freedom. The effective stochastic dynamics for the concentration of the protein biochemical species accounts for both the feedback mechanism and the role of fluctuations in the mRNA concentrations occurring on much faster time scales. An important issue in utilizing the reduction technique is to characterize the accuracy of the approximations yielding the reduced description for the specific values of ε appearing for the biochemical system. For the gene regulatory network, we explore this issue numerically in Section 7.1.1.

7.1.1. Numerical Results : Comparison of the Full Stochastic Dynamics to Reduced Stochastic Dynamics. To investigate the accuracy of the reduced stochastic dynamics of the gene regulatory network, we perform numerical studies as ε is varied. To compare the full and reduced stochastic dynamics we generate an ensemble of stochastic trajectories for the mRNA and protein concentrations. The stochastic trajectories are generated with the initial conditions $r^{\text{init}} = 0$, $V^{\text{init}} = 0$, $p^{\text{init}} = 0$, $U^{\text{init}} = 0$. The kinetics of the gene regulatory network is parameterized using the values given in Table 7.2.

As a qualitative comparison we consider the marginal probability density of the stochastic trajectories for the protein concentration for the full and reduced stochastic dynamics. To characterize at each instant in time the fluctuations of the protein concentrations, we estimated the probability density by computing a two-dimensional histogram over the ensemble when $\varepsilon = 10^{-2}$, see Figure 7.3. This shows that the mean behavior and fluctuations appear qualitatively very similar for the full and reduced stochastic dynamics. This shows that for this choice of parameters the reduction technique provides a reasonable approximation to the protein concentration fluctuations.

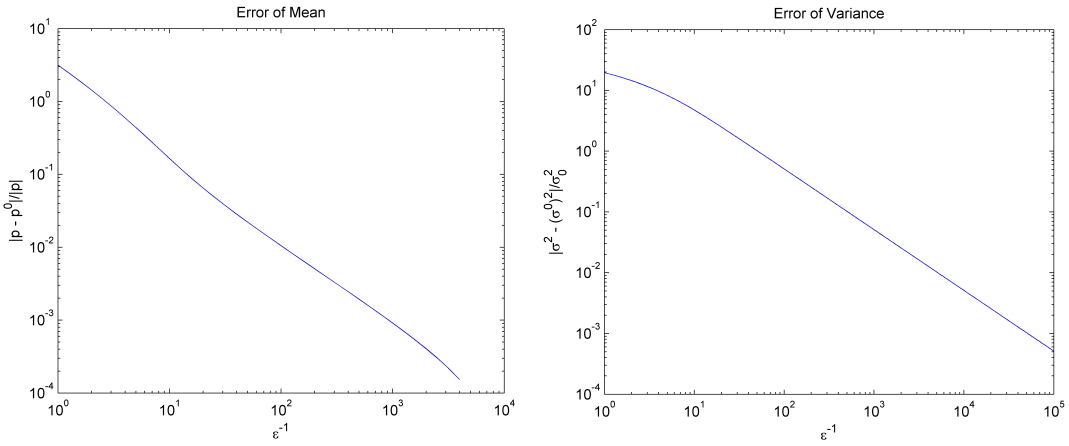

FIG. 7.4. *Relative Error of the Mean and Variance. The relative error as ε is varied is shown for the mean protein concentration using the reduced stochastic dynamics (left panel). The relative error as ε is varied for the reduced stochastic dynamics in approximating the mean behavior of the full stochastic dynamics of the protein concentration (left panel). The relative error as ε is varied for the reduced stochastic dynamics in approximating the variance of the full stochastic dynamics of the protein concentration (right panel). The* sup*-norm is used for the measure of errors over time.*

As a more quantitative comparison we consider the error in the mean and variance of the reduced stochastic dynamics in approximating the full stochastic dynamics as ε is varied. Since at each instant in time t the fluctuations in the concentrations of the protein and mRNAs are Gaussian, this serves as a measure of the error in the underlying probability distribution of the full and reduced stochastic dynamics. As a measure of the error between the mean and variance over all time the sup-norm is used. The statistics are computed from an ensemble of trajectories with the initial conditions $r^{\mathsf{init}} = 0$, $V^{\mathsf{init}} = 0$, $p^{\mathsf{init}} = 0$, $U^{\mathsf{init}} = 0$ and parameters given in Table 7.2. These results are reported in Figure 7.4.

From Figure 7.4, we see that as ε tends to zero the reduced stochastic dynamics have increasing accuracy in approximating the full stochastic dynamics for the protein concentrations. It is encouraging that even for relatively modest values of ε, on the order of 10^{-2}, the reduced stochastic dynamics yield for the mean a relative error on the order of 1%. This shows the asymptotic approximation attains a high level of accuracy for the mean behavior of the gene regulatory network, if the ratio of the mRNA and protein concentration response times is on the order 10^{-2}. In the log-log plot, the slope of the error curve is approximately one indicating the approximation converges for the mean at a rate first order in ε.

For the fluctuations of the system, it is found that a larger separation in the time scales is required to attain a comparable level of accuracy. From Figure 7.4, to achieve accuracy with a relative error of 1% requires a time scale separation having a ratio $\varepsilon = 10^{-3}$. In the log-log plot, the slope of the error curve on the right for the variance is approximately one. This indicates that the approximation converges for the variance at a rate first order in ε. This indicates that the reduction method is expected to work well even when the separation in times scale are somewhat modest, on the order of $10^{-2} - 10^{-3}$, depending on the level of accuracy sought.

7.2. An mRNA Genetic Switch for Controlling the Expression Level of Two Proteins. As a further application of the stochastic reduction technique, we consider the biochemical kinetics of a genetic system which operates like a switch to regulate the expression levels of two proteins. Specifically, we consider a system which maintains exclusively only one of the proteins at a high level of expression while keeping the other at a low level of expression. The control in this genetic switch is a third protein species whose presence or absence signals which protein to maintain at a high level.

We consider a realization of such a system with the following components: (i) two genes, (ii) two product protein species, (iii) one signaling protein species, (iv) an enzyme which cleaves molecules of mRNA, and (v)

two mRNA fragments which are capable of binding promoter sites. In our notation, we label the two genes and related products by subscripts A and B.

To obtain exclusively a high level of expression for only one protein at a time, we consider two genes which are mutually repressive. More precisely, each gene has products which act to inhibit the expression of the products of the other gene. By this mechanism only one gene will be expressed at a high level while the other is repressed. To control which of the genes is expressed, the signaling protein acts as an additional source of repression on one of the genes. This serves to break the symmetry of the system. The presence or absence of the signaling protein can be used to control which of the two possible gene products are expressed at a high level.

We now discuss some of the specific features of the kinetics we use to realize this switch mechanism. A key part of the biochemistry in our hypothesized genetic regulatory system is the cleaving of mRNA molecules which occurs between the steps of transcription and translation. This results for each mRNA molecule which is transcribed, in the production of two distinct mRNA fragments. For gene A, the uncleaved mRNA is labeled by $mRNA_A$. Each $mRNA_A$ molecule is cleaved to form two fragments labeled by $mRNA_{A1}$ and $mRNA_{A2}$. The first fragment functions as a typical mRNA molecule to be translated into the protein A. The second fragment folds into a structure which is capable of binding the promoter site of gene B. This second fragment functions to inhibit the expression of gene B. In our model, we assume similar roles for the molecules $mRNA_B$, $mRNA_{B1}$ and $mRNA_{B2}$.

To control which of the genes has a high level of expression, the protein C acts to repress expression of gene A. When protein C is present in sufficient concentration, this results in a high level of expression for gene B since very little $mRNA_{A2}$ is produced. When protein C is absent, this results in a high level of expression for gene A, since the abundant production of $mRNA_{A2}$ results in strong repression of gene B and very little $mRNA_{B2}$ is produced. This biochemical mechanism is summarized schematically in Figure 7.5.

The hypothesized genetic switch, in which mRNAs play a central role in gene regulation, was inspired by recent work on the development of synthetic nucleic acid molecules referred to as Aptamers. Aptamers have been shown to be capable of binding a wide variety of target molecules [5, 17]. The possibility that the genome might encode similar such sequences for mRNAs with the capability to bind promoter sites and perform regulatory functions has also been discussed in [5, 19, 24]. Since the repression using mRNA involves genetic products obtained before translation, such a switch is expected to result in a regulatory system capable of having a much faster response time than a regulatory system based on protein products which inhibit the genes.

To study this system, we shall use the Linear Noise Equations. We remark some care must be used for the Linear Noise Equations, since they are only valid away from the critical concentration of C which triggers switching between the expression levels of A and B. We shall consider here primarily the near-equilibrium behavior of the system in a regime where the approximations of the Linear Noise Equations are appropriate, see [30]. We discuss some specific issues for the genetic switch in more detail below.

To study the genetic switch at the level of the Linear Noise Equations, the concentrations of nine biochemical species are explicitly represented and tracked in the initial model. The nine concentrations tracked are denoted by

$$\mathbf{C} = (C_A, C_B, C_C, C_{rA}, C_{rA1}, C_{rA2}, C_{rB}, C_{rB1}, C_{rB2}), \tag{7.22}$$

where $C_{[\cdot]}$ denotes the concentration of each particular molecular species. The concentrations of the protein species are denoted by C_A, C_B, C_C, and the concentrations of the mRNA molecules and fragments by C_{rA}, C_{rA1}, C_{rA2} and C_{rB}, C_{rB1}, C_{rB2}. For notational convenience, we also denote the components by indices so that $\mathbf{C} = (C_1, \ldots, C_9)$, with the natural correspondence with the previous definition of $\mathbf{C}$.

In the Linear Noise Approximation given in equation 2.4, each of the concentrations is approximated by

$$C_k(t) \approx x_k(t) + \frac{1}{\sqrt{n}} X_k(t). \tag{7.23}$$

The x_k denotes the mean concentration of the k^{th} molecular species. The X_k denotes the fluctuations about

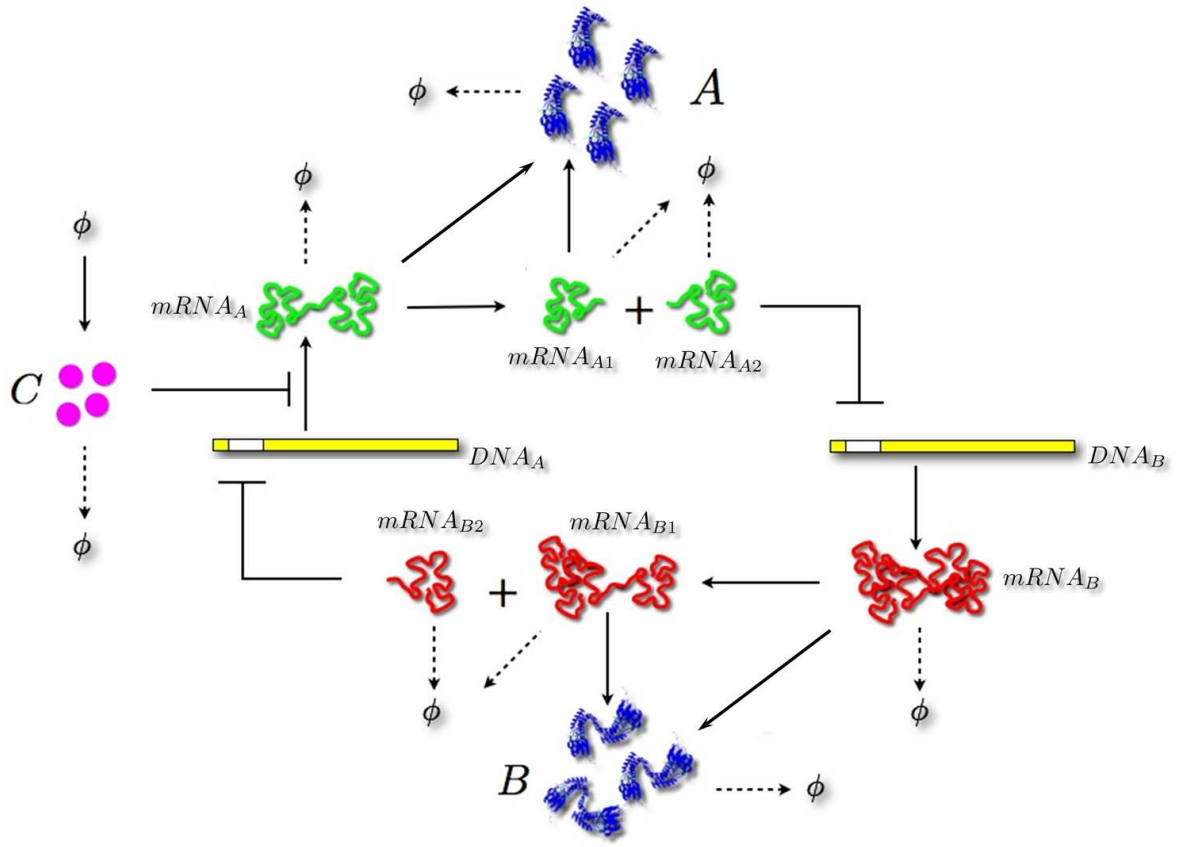

FIG. 7.5. *An mRNA genetic switch controlling the expression level of two proteins. To obtain exclusively a high level of expression for only one protein, two mutually repressive genes are considered. For gene A, molecules of $mRNA_A$ are cleaved within the nucleus by an enzyme to produce the two fragments $mRNA_{A1}$ and $mRNA_{A2}$. The first fragment $mRNA_{A1}$ is translated to protein A. The second fragment $mRNA_{A2}$ binds to the promoter site of gene B to repress its transcription. For gene B, similar roles are played by molecules of $mRNA_B$, $mRNA_{B1}$, $mRNA_{B2}$. The protein C acts to repress transcription of gene A and controls which protein is expressed at a high level. When protein C is absent, protein A is maintained at a high level of expression. When protein C is present in sufficient concentration, protein B is maintained at a high level of expression.*

the mean concentration of the k^{th} molecular species. For a more precise definition of these terms and a derivation of this approximation, see Section 2 and the equations 2.10 and 2.15.

We remark that an important consideration when using this approximation is that the concentration of protein C be sufficiently far from the critical switching threshold where the expression levels of the proteins A and B reverse roles. This is required since as the concentration of protein C approaches the switching threshold, the system becomes bistable and depends sensitively on the form of the fluctuations. In particular, the fluctuations determine which of the two possible expression levels is selected by the system. Each of these can be regarded as a metastable state. The fluctuations also play an important role in determining the time scale on which spontaneous switching occurs between these two metastable states.

For the genetic switch considered in such a regime, a more detailed description of the biochemistry is required than provided by the Linear Noise Equations and perhaps even the Chemical Masters Equations. In principle, simulation studies could be carried out by combining more detailed descriptions with the approaches to the Linear Noise Equations which we discuss here. Such hybrid approaches could be used to achieve a greater level of computational efficiency. In this spirit and to demonstrate the possible uses of

our stochastic reduction procedure, we consider here only the transient responses of the system after the switching threshold has been crossed by the concentration of protein C. We leave to other works the pursuit of such hybrid computational methods which may benefit from the studies presented here.

We now give the precise form of the kinetics used to model the regulatory switch. The kinetics for the proteins A,B,C are accounted for by the specific Linear Noise Equations

$$\dot{x}_A(t) = \kappa_{rA} x_{rA}(t) + \kappa_{rA1} x_{rA1}(t) - \gamma_A x_A(t) \tag{7.24}$$
$$\dot{x}_B(t) = \kappa_{rB} x_{rB}(t) + \kappa_{rB1} x_{rB1}(t) - \gamma_B x_B(t) \tag{7.25}$$
$$\dot{x}_C(t) = \kappa_C - \gamma_C x_C(t) \tag{7.26}$$

$$\begin{aligned} dX_A(t) &= (\kappa_A X_{rA}(t) - \gamma_A X_A(t) + \kappa_{rA1} X_{rA1}(t))\, dt \\ &\quad + (\kappa_{rA} x_{rA}(t) + \kappa_{rA1} x_{rA1}(t) + \gamma_A x_A(t))^{1/2}\, dW_A(t) \end{aligned} \tag{7.27}$$
$$\begin{aligned} dX_B(t) &= (\kappa_B X_{rB1}(t) - \gamma_B X_B(t) + \kappa_{rB1} X_{rB1}(t))\, dt \\ &\quad + (\kappa_{rB} x_{rB}(t) + \kappa_{rB1} x_{rB1}(t) + \gamma_B x_B(t))^{1/2}\, dW_B(t) \end{aligned} \tag{7.28}$$
$$dX_C(t) = -\gamma_C X_C(t) dt + (\kappa_C + \gamma_C x_C(t))^{1/2}\, dW_C(t). \tag{7.29}$$

The κ_k denotes the kinetic rate of translation of the k^{th} mRNA species to protein. The γ_k denotes the rate of degradation of molecules of the k^{th} protein species or mRNA species.

To account qualitatively for the relationship between the strength of inhibition and the concentration of molecules which bind the promoter site, we use the following functional form throughout

$$h(x, M) = \frac{1}{1 + (x/M)^N}. \tag{7.30}$$

This functional form has the property of making a transition from a value which is nearly one, for x smaller than M, to a value which is nearly zero, for x larger than M. The range of x over which this transition occurs is controlled by the exponent N. In the limit that $N \to \infty$, the functional form approaches the characteristic function for x to be less than M.

The kinetics for $mRNA_A$, $mRNA_{A1}$, $mRNA_{A2}$ are accounted for by the Linear Noise Equations

$$\dot{x}_{rA}(t) = \frac{1}{\varepsilon}\left(k_{rA}^{\mathsf{max}} h(x_C(t), M_C) h(x_{rB2}(t), M_{rB2}) - \gamma_{rA} x_{rA}(t) - k_{rA}^{\mathsf{cl}} x_{rA}(t)\right) \tag{7.31}$$

$$\dot{x}_{rA1}(t) = \frac{1}{\varepsilon}\left(k_{rA}^{\mathsf{cl}} x_{rA}(t) - \gamma_{rA1} x_{rA1}(t)\right) \tag{7.32}$$

$$\dot{x}_{rA2}(t) = \frac{1}{\varepsilon}\left(k_{rA}^{\mathsf{cl}} x_{rA}(t) - \gamma_{rA2} x_{rA2}(t)\right) \tag{7.33}$$

$$\begin{aligned} dX_{rA}(t) = \frac{1}{\varepsilon}\Bigg(& k_{rA}^{\mathsf{max}} \frac{\partial h}{\partial x}(x_C(t), M_C) h(x_{rB2}(t), M_{rB2}) X_C(t) \\ & - (\gamma_{rA} + k_{rA}^{\mathsf{cl}}) X_{rA}(t) + k_{rA}^{\mathsf{max}} h(x_C(t), M_C) \frac{\partial h}{\partial x}(x_{rB2}(t), M_{rB2}) X_{rB2}(t) \Bigg) dt \\ & + \frac{1}{\sqrt{\varepsilon}}\left(k_{rA}^{\mathsf{max}} h(x_A(t), M_{rA}) h(x_{rB2}(t), M_{rB2}) + \gamma_{rA} x_{rA}(t) + k_A^{\mathsf{cl}} x_{rA}(t)\right)^{1/2} dW_{rA}(t) \end{aligned} \tag{7.34}$$

$$\begin{aligned} dX_{rA1}(t) = & \frac{1}{\varepsilon}\left(k_{rA}^{\mathsf{cl}} X_{rA}(t) - \gamma_{rA1} X_{rA1}(t)\right) dt \\ & + \frac{1}{\sqrt{\varepsilon}}\left(k_{rA}^{\mathsf{cl}} x_{rA}(t) + \gamma_{rA1} x_{rA1}(t)\right)^{1/2} dW_{rA1}(t) \end{aligned} \tag{7.35}$$

$$\begin{aligned} dX_{rA2}(t) = & \frac{1}{\varepsilon}\left(k_{rA}^{\mathsf{cl}} X_{rA}(t) - \gamma_{rA2} X_{rA2}(t)\right) dt \\ & + \frac{1}{\sqrt{\varepsilon}}\left(k_{rA}^{\mathsf{cl}} x_{rA}(t) + \gamma_{rA2} x_{rA2}(t)\right)^{1/2} dW_{rA2}(t). \end{aligned} \tag{7.36}$$

The ϵ is a characteristic time-scale over which reactions occur for the $mRNA_A$ molecules. The k_{rA}^{max} denotes the maximum rate of transcription of $mRNA_A$. The k_{rA}^{cl} denotes the rate at which molecules of $mRNA_A$ are cleaved to form the two fragments $mRNA_{A1}$ and $mRNA_{A2}$. To account for the inhibition arising from the binding of $mRNA_{B2}$ and protein C to the promoter site of gene A, we use the functional form defined in equation 7.30 and the threshold constants M_{rB2}, M_C. Degradation of the mRNA molecules is accounted for by the rate constants γ_{rA}, γ_{rA1}, and γ_{rA2}.

The kinetics for $mRNA_B$, $mRNA_{B1}$, $mRNA_{B2}$ are accounted for by the Linear Noise Equations

$$\dot{x}_{rB}(t) = \frac{1}{\varepsilon}\left(k_{rB}^{\mathsf{max}} h(x_{rA2}(t), M_{rA2}) - \gamma_{rB} x_{rB}(t) - k_{rB}^{\mathsf{cl}} x_{rB}(t)\right) \tag{7.37}$$

$$\dot{x}_{rB1}(t) = \frac{1}{\varepsilon}\left(k_{rB}^{\mathsf{cl}} x_{rB}(t) - \gamma_{rB1} x_{rB1}(t)\right) \tag{7.38}$$

$$\dot{x}_{rB2}(t) = \frac{1}{\varepsilon}\left(k_{rB}^{\mathsf{cl}} x_{rB}(t) - \gamma_{rB2} x_{rB2}(t)\right) \tag{7.39}$$

$$dX_{rB}(t) = \frac{1}{\varepsilon}\left(k_{rB}^{\mathsf{max}} \frac{\partial h}{\partial x}(x_{rA2}(t), M_{rA2}) X_{rA2}(t) - (\gamma_{rB} + k_{rB}^{\mathsf{cl}}) X_{rB}(t)\right) dt \tag{7.40}$$

$$+ \frac{1}{\sqrt{\varepsilon}}\left(k_{rB}^{\mathsf{max}} h(x_{rA2}(t), M_{rA2}) + (\gamma_{rB} + k_{rB}^{\mathsf{cl}}) x_{rB}(t)\right)^{1/2} dW_{rB}(t) \tag{7.41}$$

$$dX_{rB1}(t) = \frac{1}{\varepsilon}\left(k_{rB}^{\mathsf{cl}} X_{rB}(t) - \gamma_{rB1} X_{rB1}(t)\right) dt \tag{7.42}$$

$$+ \frac{1}{\sqrt{\varepsilon}}\left(k_{rB}^{\mathsf{cl}} x_{rB}(t) + \gamma_{rB1} x_{rB1}(t)\right)^{1/2} dW_{rB1}(t) \tag{7.43}$$

$$dX_{rB2}(t) = \frac{1}{\varepsilon}\left(k_{rB}^{\mathsf{cl}} X_{rB}(t) - \gamma_{rB2} X_{rB2}(t)\right) dt \tag{7.44}$$

$$+ \frac{1}{\sqrt{\varepsilon}}\left(k_{rB}^{\mathsf{cl}} x_{rB}(t) + \gamma_{rB2} x_{rB2}(t)\right)^{1/2} dW_{rB2}(t). \tag{7.45}$$

The ϵ is a characteristic time-scale over which reactions occur for the $mRNA_B$ molecules. The k_{rB}^{max} denotes the maximum rate of transcription of $mRNA_B$. The k_{rB}^{cl} denotes the rate at which molecules of $mRNA_B$ are cleaved to form the two fragments $mRNA_{B1}$ and $mRNA_{B2}$. To account for the inhibition arising from the binding of $mRNA_{A2}$ to the promoter site of gene B, we use the functional form defined in equation 7.30 and the threshold constants M_{rA2}. Degradation of the mRNA molecules is accounted for by the rate constants γ_{rB}, γ_{rB1}, and γ_{rB2}. A key difference of between the $mRNA_B$ kinetics compared to those for $mRNA_A$ is the absence of the inhibition term involving protein C. In the genetic switch considered, the signaling protein C only influences the transcription rate of $mRNA_A$.

An important feature of the regulatory mechanism of the switch is that the mutual inhibition occurs through the mRNA molecules before translation. As a consequence, it is expected the part of the biochemical kinetics responsible for controlling the switch will primarily occur on much faster time scales than the biochemical kinetics associated with the proteins. To exploit this feature, we shall use the stochastic reduction technique introduced in Section 4. This will allow for a model to be derived which is formulated completely in terms of the concentrations of protein A, protein B, and protein C.

We use the reduction procedure to obtain effective equations for the proteins both for the mean concentrations and for the fluctuations in the concentrations. The following reduced system of differential-algebraic

equations are obtained for the effective dynamics of the mean concentration of the proteins

$$\dot{x}^0_{_A}(t) = \kappa_{_A} x^0_{_{rA}}(t) + \kappa_{_{rA1}} x^0_{_{rA1}}(t) - \gamma_{_A} x^0_{_A}(t) \tag{7.46}$$
$$\dot{x}^0_{_B}(t) = \kappa_{_B} x^0_{_{rB}}(t) + \kappa_{_{rB1}} x^0_{_{rB1}}(t) - \gamma_{_B} x^0_{_B}(t) \tag{7.47}$$
$$\dot{x}^0_{_C}(t) = \kappa_{_C} - \gamma_{_C} x^0_{_C}(t) \tag{7.48}$$

$$x^0_{_{rA}}(t) = \Gamma(x^0_{_C}(t)) \tag{7.49}$$
$$x^0_{_{rA1}}(t) = \frac{k^{\mathsf{cl}}_{_{rA}}}{\gamma_{_{rA1}}} \Gamma(x^0_{_C}(t)) \tag{7.50}$$
$$x^0_{_{rA2}}(t) = \frac{k^{\mathsf{cl}}_{_{rA}}}{\gamma_{_{rA2}}} \Gamma(x^0_{_C}(t)) \tag{7.51}$$
$$x^0_{_{rB}}(t) = \frac{k^{\mathsf{max}}_{_{rB}}}{\gamma_{_{rB}} + k^{\mathsf{cl}}_{_{rB}}} h\left(\frac{k^{\mathsf{cl}}_{_{rA}}}{\gamma_{_{rA2}}} \Gamma(x^0_{_C}(t)), M_{_{rA2}} \right) \tag{7.52}$$
$$x^0_{_{rB1}}(t) = \frac{k^{\mathsf{cl}}_{_{rB}}}{\gamma_{_{rB1}}} \frac{k^{\mathsf{max}}_{_{rB}}}{(\gamma_{_{rB}} + k^{\mathsf{cl}}_{_{rB}})} h\left(\frac{k^{\mathsf{cl}}_{_{rA}}}{\gamma_{_{rA2}}} \Gamma(x^0_{_C}(t)), M_{_{rA2}} \right) \tag{7.53}$$
$$x^0_{_{rB2}}(t) = \frac{k^{\mathsf{cl}}_{_{rB}}}{\gamma_{_{rB2}}} \frac{k^{\mathsf{max}}_{_{rB}}}{(\gamma_{_{rB}} + k^{\mathsf{cl}}_{_{rB}})} h\left(\frac{k^{\mathsf{cl}}_{_{rA}}}{\gamma_{_{rA2}}} \Gamma(x^0_{_C}(t)), M_{_{rA2}} \right). \tag{7.54}$$

The term $\Gamma = \Gamma(x_{_C})$ denotes the solution to the following implicit equation

$$(\gamma_{_{rA}} + k^{\mathsf{cl}}_{_{rA}})\Gamma - k^{\mathsf{max}}_{_{rA}} h(x_{_C}, M_{_C}) h\left(\frac{k^{\mathsf{cl}}_{_{rB}}}{\gamma_{_{rB2}}} \frac{k^{\mathsf{max}}_{_{rB}}}{(\gamma_{_{rB}} + k^{\mathsf{cl}}_{_{rB}})} h\left(\frac{k^{\mathsf{cl}}_{_{rA}}}{\gamma_{_{rA2}}} \Gamma, M_{_{rA2}} \right), M_{_{rB2}} \right) = 0. \tag{7.55}$$

The following reduced system of stochastic differential equations are obtained for the effective dynamics of the fluctuations for the protein concentrations

$$d\mathbf{Z}^0(t) = B(t)\mathbf{Z}^0(t)dt + \boldsymbol{\sigma}^0(t)d\mathbf{W}(t) \tag{7.56}$$

where $\mathbf{Z}^0(t) = (X_{_A}(t), X_{_A}(t), X_{_C}(t))$ and $d\mathbf{W}$ denotes increments of Brownian motion in $\mathbb{R}^3$. The operator B obtained in the reduction procedure is given by

$$B(t) = D_{\mathsf{s}} F_{\mathsf{s}}(\mathbf{x}^0(t)) - D_{\mathsf{f}} F_{\mathsf{s}}(\mathbf{x}^0(t)) [D_{\mathsf{f}} F_{\mathsf{f}}(\mathbf{x}^0(t))]^{-1} D_{\mathsf{s}} F_{\mathsf{f}}(\mathbf{x}^0(t)). \tag{7.57}$$

For the genetic switch, this is given by the following specific terms

$$D_{\mathsf{s}}F_{\mathsf{s}}(\mathbf{x}) = \begin{bmatrix} -\gamma_A & 0 & 0 \\ 0 & -\gamma_B & 0 \\ 0 & 0 & -\gamma_C \end{bmatrix}$$

$$D_{\mathsf{f}}F_{\mathsf{s}}(\mathbf{x}) = \begin{bmatrix} \kappa_A & \kappa_{rA1} & 0 & 0 & 0 & 0 \\ 0 & 0 & 0 & \kappa_B & \kappa_{rB1} & 0 \\ 0 & 0 & 0 & 0 & 0 & 0 \end{bmatrix}$$

$$D_{\mathsf{s}}F_{\mathsf{f}}(\mathbf{x}) = \begin{bmatrix} 0 & 0 & k_{rA}^{\mathsf{max}} \frac{\partial h}{\partial x}(x_C, M_C) h(x_{rB2}, M_{rB2}) \\ 0 & 0 & 0 \\ 0 & 0 & 0 \\ 0 & 0 & 0 \\ 0 & 0 & 0 \\ 0 & 0 & 0 \end{bmatrix}$$

$$D_{\mathsf{f}}F_{\mathsf{f}}(\mathbf{x}) = \begin{bmatrix} -(\gamma_{rA} + k_{rA}^{\mathsf{cl}}) & 0 & 0 & 0 & 0 & k_{rA}^{\mathsf{max}} h(x_C, M_C) \frac{\partial h}{\partial x}(x_{rB2}, M_{rB2}) \\ k_{rA}^{\mathsf{cl}} & -\gamma_{rA1} & 0 & 0 & 0 & 0 \\ k_{rA}^{\mathsf{cl}} & 0 & -\gamma_{rA2} & 0 & 0 & 0 \\ 0 & 0 & k_{rB}^{\mathsf{max}} \frac{\partial h}{\partial x}(x_{rA2}, M_{rA2}) & -(\gamma_{rB} + k_{rB}^{\mathsf{cl}}) & 0 & 0 \\ 0 & 0 & 0 & k_{rB}^{\mathsf{cl}} & -\gamma_{rB1} & 0 \\ 0 & 0 & 0 & k_{rB}^{\mathsf{cl}} & 0 & -\gamma_{rB2} \end{bmatrix}. \tag{7.58}$$

From equation 7.57 and 7.58, the operator $B(t)$ can be computed readily at each time t. For the genetic switch, the term $\boldsymbol{\sigma}^0(t)$ for the fluctuations in the reduced equations is given by

$$\boldsymbol{\sigma}^0 = \begin{bmatrix} \sigma_A^0 & 0 & 0 \\ 0 & \sigma_B^0 & 0 \\ 0 & 0 & \sigma_C^0 \end{bmatrix} \tag{7.59}$$

where

$$\sigma_A^0(t) = \sqrt{\kappa_{rA} x_{rA}^0(t) + \kappa_{rA1} x_{rA1}^0(t) + \gamma_A x_A^0(t)} \tag{7.60}$$

$$\sigma_B^0(t) = \sqrt{\kappa_{rB} x_{rB}^0(t) + \kappa_{rB1} x_{rB1}^0(t) + \gamma_B x_B^0(t)} \tag{7.61}$$

$$\sigma_C^0(t) = \sqrt{(\kappa_C + \gamma_C) x_C^0(t)}. \tag{7.62}$$

This determines for the genetic switch a closed set of equations for the effective stochastic dynamics of the concentration of the proteins A, B, C. To help characterize the quality of this reduced approximation of the full system of Linear Noise Equations, we carry-out numerical studies by varying ϵ to compare the reduced model to the full model.

7.2.1. Numerical Results: Comparison of the full stochastic dynamics with the reduced stochastic dynamics. To investigate the accuracy of the reduced stochastic dynamics of the genetic switch, we perform numerical studies as ε is varied. To compare the full and reduced stochastic dynamics we generate an ensemble of stochastic trajectories for the full set of concentrations for both the mRNAs and proteins. The stochastic trajectories are generated with the parameter values given in Table 7.3.

As a qualitative comparison, we consider the marginal probability density of the stochastic trajectories for the protein concentrations for the full and reduced stochastic dynamics. To characterize at each instant in time the fluctuations in concentration of each protein species, we estimated the probability density by computing a two-dimensional histogram over the ensemble when $\varepsilon = 10^{-2}$, see Figures 7.6 and 7.7. The results for protein C are not reported since its dynamics are retained exactly in the reduction and the error is always zero. For protein A and protein B, the figures show that the behavior both of the mean and of the fluctuations are for the reduced stochastic dynamics very similar to the full stochastic dynamics. This

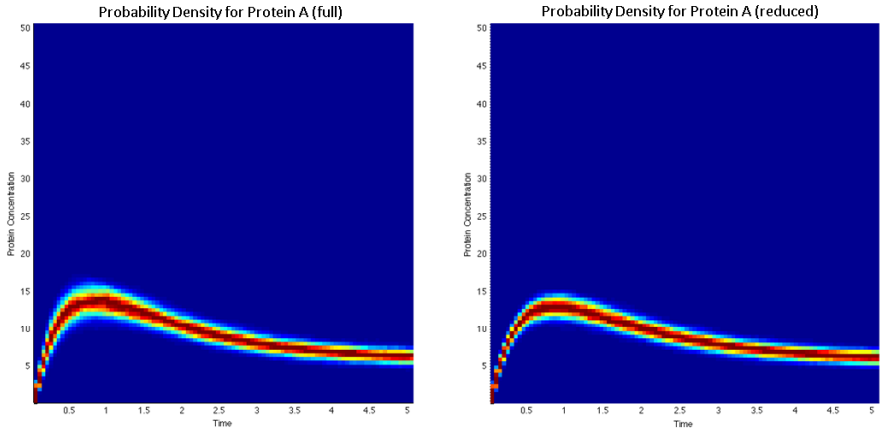

FIG. 7.6. *Comparison of the marginal probability density of the full and reduced stochastic dynamics for the genetic switch.*

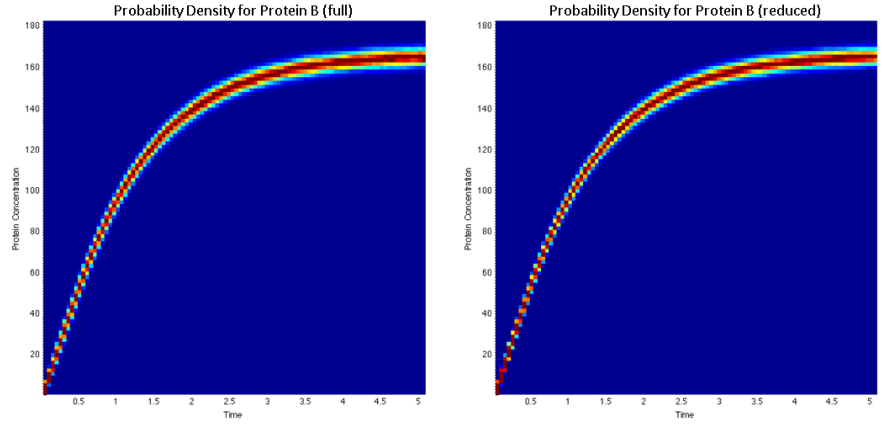

FIG. 7.7. *Comparison of the marginal probability density of the full and reduced stochastic dynamics for the genetic switch.*

indicates that for this choice of parameters the reduction technique provides a reasonable approximation for the trends and fluctuations of the protein concentration.

As a more quantitative comparison, we consider as ε is varied the error in the mean and variance of the reduced stochastic dynamics in approximating the full stochastic dynamics. Since at each instant in time the fluctuations in the concentrations of the proteins and mRNAs are Gaussian, this serves as a measure of the error in the underlying probability distribution of the full and reduced stochastic dynamics. As a measure of the error between the mean and variance over all time, the sup-norm is used. The statistics are computed from an ensemble of trajectories generated with the parameters given in Table 7.3. These results are reported in Figures 7.8. We remark that the results for protein C are not reported since its dynamics are retained exactly in the reduction and the error is always zero.

From Figure 7.8, we see that as ε tends to zero the reduced stochastic dynamics has increasing accuracy in approximating the full stochastic dynamics for the protein concentrations. It is encouraging that even for relatively modest values of ε, on the order of 10^{-1}, the reduced stochastic dynamics yield for the mean a relative error on the order of 1%. This shows the asymptotic approximation attains a high level of accuracy for the mean behavior of the genetic switch, even if the ratio of the mRNA and protein concentration response times is only on the order 10^{-1}. In the log-log plot, the slope of the error curve is approximately one indicating the approximation converges for the mean at a rate first order in ε.

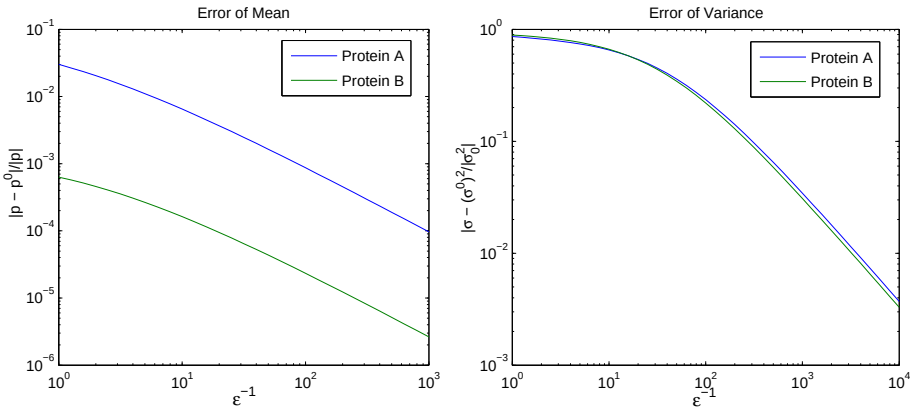

FIG. 7.8. *Relative error of the mean and variance of the stochastic dynamics of the reduced model when approximating the full model. The sup-norm is used to measure the error over time.*

For the fluctuations of the proteins of the genetic switch, it is found that a larger separation in the time scales is required to attain a comparable level of accuracy. From Figure 7.8, it is seen that to achieve accuracy with a relative error of 1% requires a time scale separation having a ratio $\varepsilon = 10^{-3}$. In the log-log plot, the slope of the error curve on the right for the variance is approximately one. This indicates that the approximation converges for the variance at a rate first order in ε. This indicates that the reduction method is expected to work well when the separation in times scale is on the order of $10^{-3} - 10^{-4}$, of course this depends on the level of accuracy sought.

These results show that for the genetic switch, some of the detailed kinetics responsible for the switching mechanism can be replaced by appropriate functional forms in the protein equations. The empirical results reported here give an indication of the actual magnitudes in the separation of time scales which are required in practice to attain a given level of accuracy in such approximations.

8. Conclusion. A systematic approach was presented for obtaining reduced models to approximate the full stochastic dynamics of biochemical concentrations described by the Linear Noise Equations. The reduced model is obtained by explicitly representing only the chemical species having dynamics with relatively slow characteristic time scales while eliminating representations of the chemical species having dynamics with relatively fast characteristic time scales. Effective stochastic dynamics for the slow chemical species is obtained through a singular perturbation analysis of the Backward Kolomogorov PDEs for the Linear Noise Equations. The multiscale reduction technique is demonstrated in the context of gene regulatory networks. It is found that even for relatively modest separation in time scales, the reduced model offers a reasonable approximation of the full stochastic dynamics. The presented stochastic reduction procedure provides a potentially versatile tool for systematically obtaining reduced approximations of Linear Noise Equations.

9. Acknowledgements. The author C.P. was supported by Department of Mathematics, Visiting Assistant Professor (VAP) position at UCSB. The author P.J.A was supported by NSF Mathematical Biology Grant DMS - 0635535 and NSF CAREER Grant DMS - 0956210. The author M.K. acknowledges research funding from NSF through Grants ECCS-0835847 and ECCS-0802008 and funding from the Institute for Collaborative Biotechnologies through Grant DAAD19-03-D-0004 from the US Army Research Office.

REFERENCES

[1] URI ALON, *An Introduction to Systems Biology. Design Principles of Biological Circuits.*, Chapman & Hall/CRC., 2007.
[2] ADAM ARKIN, JOHN ROSS, AND HARLEY H. MCADAMS, *Stochastic kinetic analysis of developmental pathway bifurcation in phage lambda-infected escherichia coli cells*, Genetics, 149 (1998), pp. 1633–1648.
[3] P. J. ATZBERGER, *A note on the correspondence of an immersed boundary method incorporating thermal fluctuations with stokesian-brownian dynamics*, Physica D-Nonlinear Phenomena, 226 (2007), pp. 144–150–.

[4] B.Alberts, A.Johnson, J.Lewis, M.Raff, K.Roberts, and P.Walter, *Molecular Biology of the Cell*, Garland Publishing, 2002.
[5] David H. J. Bunka and Peter G. Stockley, *Aptamers come of age at last*, Nat Rev Micro, 4 (2006), pp. 588–596.
[6] Yang Cao, Daniel T. Gillespie, and Linda R. Petzold, *The slow-scale stochastic simulation algorithm*, The Journal of Chemical Physics, 122 (2005), p. 014116.
[7] Weinan E, Di Liu, and Eric Vanden-Eijnden, *Nested stochastic simulation algorithms for chemical kinetic systems with multiple time scales*, Journal of Computational Physics, 221 (2007), pp. 158–180.
[8] J. Elf and M. Ehrenberg, *Fast evaluation of fluctuations in biochemical networks with the linear noise approximation*, Genome Research, 13 (2003), pp. 2475–2484.
[9] Stewart N. Ethier and Thomas G. Kurtz, *Markov Processes: Characterization and Convergence.*, John Wiley & Sons Inc., 1986.
[10] Daniel Forger, Didier Gonze, David Virshup, and David K. Welsh, *Beyond intuitive modeling: Combining biophysical models with innovative experiments to move the circadian clock field forward*, J Biol Rhythms, 22 (2007), pp. 200–210.
[11] C. W. Gardiner, *Handbook of stochastic methods: for Physics, Chemistry, and the Natural Sciences*, Springer Series in Synergetics, Springer-Verlag, second edition ed., 1997.
[12] Daniel T. Gillespie, *A rigorous derivation of the chemical master equation*, Physica A: Statistical Mechanics and its Applications, 188 (1992), pp. 404–425.
[13] Eric L. Haseltine and James B. Rawlings, *Approximate simulation of coupled fast and slow reactions for stochastic chemical kinetics*, The Journal of Chemical Physics, 117 (2002), pp. 6959–6969.
[14] M. Holmes, *Introduction to Perturbation Methods*, Springer-Verlag, 1995.
[15] Thomas G. Kurtz, *A limit theorem for perturbed operator semigroups with applications to random evolutions*, Journal of Functional Analysis, 12 (1973), pp. 55–67.
[16] Reinhard Lipowsky, Yan Chai, Stefan Klumpp, Steffen Liepelt, and Melanie J.I. Mller, *Molecular motor traffic: From biological nanomachines to macroscopic transport*, Physica A: Statistical Mechanics and its Applications, 372 (2006), pp. 34–51.
[17] Xinhui Lou, Jiangrong Qian, Yi Xiao, Lisan Viel, Aren E. Gerdon, Eric T. Lagally, Paul Atzberger, Theodore M. Tarasow, Alan J. Heeger, and H. Tom Soh, *Micromagnetic selection of aptamers in microfluidic channels*, Proceedings of the National Academy of Sciences, 106 (2009), pp. 2989–2994.
[18] A. J. Majda, I. Timofeyev, and E. Vanden Eijnden, *A mathematical framework for stochastic climate models*, Communications on Pure and Applied Mathematics, 54 (2001), pp. 891–974.
[19] Maumita Mandal and Ronald R. Breaker, *Gene regulation by riboswitches*, Nat Rev Mol Cell Biol, 5 (2004), pp. 451–463.
[20] Nicholas Metropolis and S. Ulam, *The monte carlo method*, Journal of the American Statistical Association, 44 (Sep., 1949), pp. 335–341.
[21] B. Oksendal, *Stochastic Differential Equations: An Introduction*, Springer, 2000.
[22] Johan Paulsson and Mans Ehrenberg, *Random signal fluctuations can reduce random fluctuations in regulated components of chemical regulatory networks*, Phys. Rev. Lett., 84 (2000), pp. 5447–.
[23] Slaven Peles, Brian Munsky, and Mustafa Khammash, *Reduction and solution of the chemical master equation using time scale separation and finite state projection*, The Journal of Chemical Physics, 125 (2006), p. 204104.
[24] Arjun Raj, *(private communication)*.
[25] Christopher V. Rao and Adam P. Arkin, *Stochastic chemical kinetics and the quasi-steady-state assumption: Application to the gillespie algorithm*, The Journal of Chemical Physics, 118 (2003), pp. 4999–5010.
[26] Michael Reed and Barry Simon, *Functional Analysis*, Elsevier, 1980.
[27] Sheldon M. Ross, *Stochastic Processes*, John Wiley & Sons Inc., 1996.
[28] Carine Rosse, Mark Linch, Stephanie Kermorgant, Angus J. M. Cameron, Katrina Boeckeler, and Peter J. Parker, *Pkc and the control of localized signal dynamics*, Nat Rev Mol Cell Biol, 11 (2010), pp. 103–112.
[29] Giorgio Scita and Pier Paolo Di Fiore, *The endocytic matrix*, Nature, 463 (2010), pp. 464–473.
[30] N. G. van Kampen, *Stochastic Processes in Physics and Chemistry*, Elsevier, 2007.

Parameter	Description
k_p	Rate of production of Protein.
γ_p	Rate of degradation of Protein.
$\varepsilon^{-1}k_r^{\max}$	Maximum Rate of production of mRNA.
$\varepsilon^{-1}\gamma_r$	Rate of degradation of mRNA.
ε	Scaling parameter.
K_D	Parameter in Hill coefficient.
N	Hill coefficient.
n	Reaction volume.

TABLE 7.1
Description of the parameters and notation.

Parameter	Value
k_p	10hr^{-1}.
γ_p	1hr^{-1}.
k_r^{max}	10.
γ_r	1.
ε	$10^{-4}\text{s} - 1\text{s}$.
K_D	60.
N	4.
n	25.

TABLE 7.2
Values used for the parameters.

Parameter	Description	Value
κ_{rA}	Translation rate of protein A from $\mathsf{mRNA_A}$.	5
κ_{rA1}	Translation rate of protein A from $\mathsf{mRNA_{A1}}$.	10
κ_{rB}	Translation rate of protein B from $\mathsf{mRNA_B}$.	5
κ_{rB1}	Translation rate of protein B from $\mathsf{mRNA_{B1}}$.	10
κ_C	Production rate of protein C.	20
k_{rA}^{max}	Maximum transcription rate of $\mathsf{mRNA_A}$.	20
k_{rB}^{max}	Maximum transcription rate of $\mathsf{mRNA_B}$.	20
k_{rA}^{cl}	Cleaving rate of $\mathsf{mRNA_A}$.	2
k_{rB}^{cl}	Cleaving rate of $\mathsf{mRNA_B}$.	2
M_{rA2}	Repression threshold.	6
M_{rB2}	Repression threshold.	6
M_C	Repression threshold.	10
γ_k	Rate of degradation of the k^{th} molecular species.	1
N	Hill coefficient.	2
n	Volume.	25
ε	Time-scale separation parameter (ratio of time-scales).	10^{-3} to 1

TABLE 7.3
Values used for the parameters.